iScience

CellPress
OPEN ACCESS

Article

Weight loss and cystic disease progression in autosomal dominant polycystic kidney disease

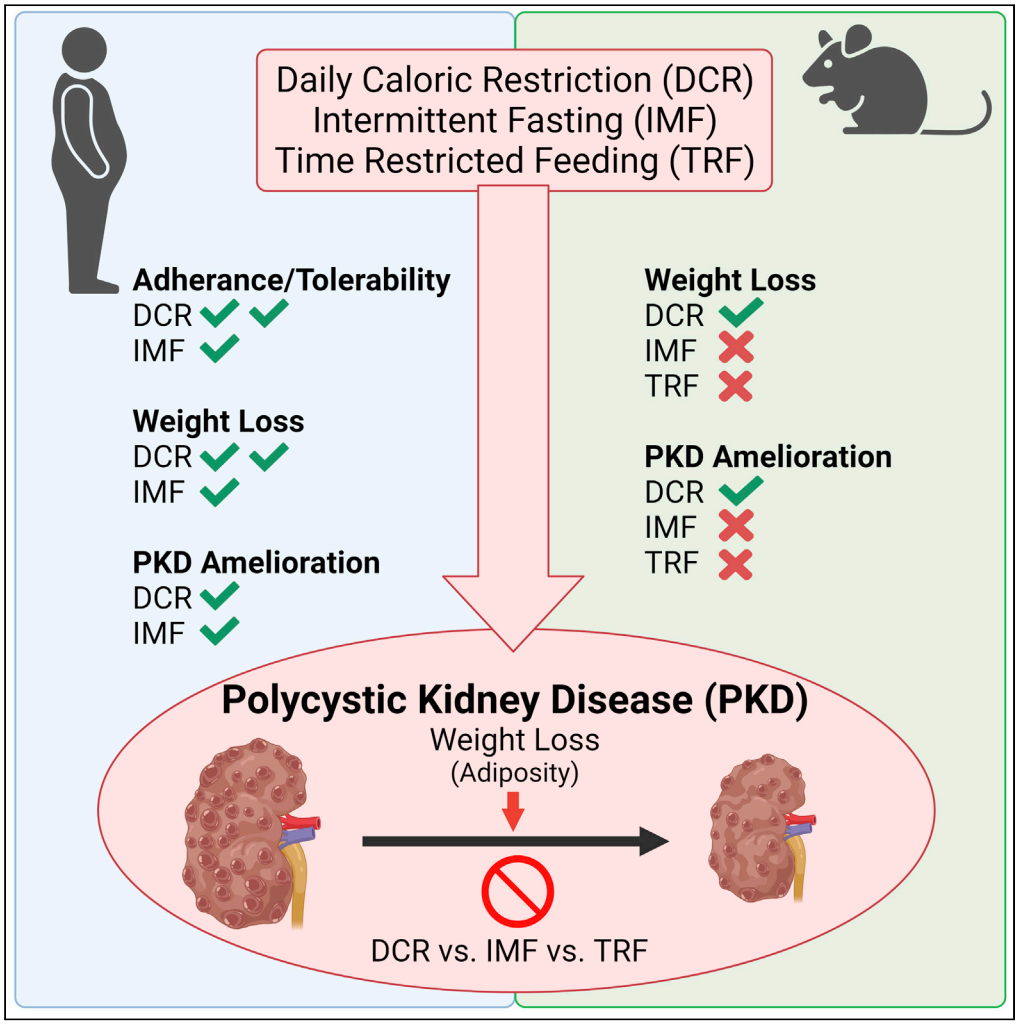

Katharina Hopp, Victoria A. Catenacci, Nidhi Dwivedi, ..., Berenice Gitomer, Michel Chonchol, Kristen L. Nowak

katharina.hopp@cuanschutz.edu (K.H.)
kristen.nowak@cuanschutz.edu (K.L.N.)

Highlights

Daily/intermittent caloric reduction is feasible in overweight/obese ADPKD patients

Daily versus intermittent caloric reduction resulted in better weight loss/adherence

In ADPKD mice, daily but not timed or intermitted fasting caused weight loss

Weight loss correlated with slowed cyst growth in ADPKD patients and mice

Hopp et al., iScience 25, 103697
January 21, 2022
https://doi.org/10.1016/j.isci.2021.103697

iScience

CellPress
OPEN ACCESS

Article

Weight loss and cystic disease progression in autosomal dominant polycystic kidney disease

Katharina Hopp,[1,2,*] Victoria A. Catenacci,[3] Nidhi Dwivedi,[1] Timothy L. Kline,[4,5] Wei Wang,[1] Zhiying You,[1] Dustin T. Nguyen,[1] Kristen Bing,[3] Bhavya Poudyal,[4] Ginger C. Johnson,[3] Matthew R. Jackman,[3] Marsha Miller,[3] Cortney N. Steele,[1] Natalie J. Serkova,[6] Paul S. MacLean,[3] Raphael A. Nemenoff,[1,2] Berenice Gitomer,[1] Michel Chonchol,[1,2] and Kristen L. Nowak[1,7,*]

SUMMARY

Progression of autosomal dominant polycystic kidney disease (ADPKD) is modified by metabolic defects and obesity. Indeed, reduced food intake slows cyst growth in preclinical rodent studies. Here, we demonstrate the feasibility of daily caloric restriction (DCR) and intermittent fasting (IMF) in a cohort of overweight or obese patients with ADPKD. Clinically significant weight loss occurred with both DCR and IMF; however, weight loss was greater and adherence and tolerability were better with DCR. Further, slowed kidney growth correlated with body weight and visceral adiposity loss independent of dietary regimen. Similarly, we compared the therapeutic efficacy of DCR, IMF, and time restricted feeding (TRF) using an orthologous ADPKD mouse model. Only ADPKD animals on DCR lost significant weight and showed slowed cyst growth compared to *ad libitum*, IMF, or TRF feeding. Collectively, this supports therapeutic feasibility of caloric restriction in ADPKD, with potential efficacy benefits driven by weight loss.

INTRODUCTION

Autosomal dominant polycystic kidney disease (ADPKD) is the most common life-threatening genetic kidney disease and is characterized by progressive development and enlargement of kidney cysts, leading to end-stage kidney disease (Torres et al., 2007; Chapman et al., 2003). In recent years, it has been suggested that lifestyle choices may be significant modulators of disease progression. One such example is overweight and obesity which, similar to the general population, is rising in prevalence in patients with ADPKD (Helal et al., 2013). We have reported that overweight, and particularly obesity, are strong independent predictors of ADPKD progression, including kidney growth, measured as change in total kidney volume (TKV) by magnetic resonance imaging (MRI) (Nowak et al., 2018, 2021).

Further, accumulating evidence supports that metabolic dysregulation impacts ADPKD progression (Nowak and Hopp, 2020). A multitude of dietary interventions aimed to correct metabolic defects have been tested in non-ADPKD rodent models or humans. These include daily caloric restriction (DCR) consisting of a reduction in daily caloric intake (e.g., 30% restriction daily), time restricted feeding (TRF) consisting of limiting caloric intake to a narrow time interval each day (e.g., 8 h/day), and intermittent fasting (IMF) consisting of fasting or substantially reducing caloric intake (e.g., 20% of caloric needs for weight maintenance one to three non-consecutive days per week). While non-ADPKD preclinical studies have focused on the mechanistic aspects of these dietary regimens in prolonging health span and alleviating disease, non-ADPKD human studies have focused on feasibility and compliance (Nowak and Hopp, 2020). Indeed, recent studies in animal models of ADPKD have shown that DCR profoundly slows kidney cyst growth and maintains kidney function (Warner et al., 2016; Kipp et al., 2016). TRF without caloric reduction was also shown to slow kidney cyst growth via induction of ketosis (Torres et al., 2019). Thus, it is plausible that weight loss, caloric restriction, and/or periods of fasting may be beneficial in slowing ADPKD progression in humans. However, the feasibility of these behavioral dietary interventions in an ADPKD patient cohort, and whether the driver of therapeutic efficacy is periods of fasting or reduction in body weight, either dependent or independent of metabolic reprogramming, remains unclear.

[1]Department of Medicine, Division of Renal Diseases and Hypertension, University of Colorado Anschutz Medical Campus, Aurora, CO 80045, USA

[2]Consortium for Fibrosis Research and Translation, University of Colorado Anschutz Medical Campus, Aurora, CO 80045, USA

[3]Department of Medicine, Division of Endocrinology, University of Colorado Anschutz Medical Campus, Aurora, CO 80045, USA

[4]Department of Radiology, Mayo Clinic College of Medicine, Rochester, MN 55901, USA

[5]Division of Nephrology and Hypertension, Mayo Clinic College of Medicine, Rochester, MN 55901, USA

[6]Department of Radiology, University of Colorado Anschutz Medical Campus, Aurora, CO 80045, USA

[7]Lead contact

*Correspondence: katharina.hopp@cuanschutz.edu (K.H.), kristen.nowak@cuanschutz.edu (K.L.N.)

https://doi.org/10.1016/j.isci.2021.103697

Accordingly, we designed a one-year behavioral weight loss intervention feasibility study, based on either DCR or IMF in adults with overweight or obesity and ADPKD with normal to moderately declined kidney function. We complemented this study with a preclinical murine trial conducted in parallel using an ADPKD1 model, which allowed us to expand the dietary regimens tested to include TRF, study the effects of dietary intake in the setting of normal body weight, and begin to evaluate signaling cascades impacted by the dietary regimens. Importantly, in both the preclinical and clinical study, the targeted weekly energy deficit was designed to be similar (~34%) between groups (DCR versus IMF or TRF) and models (human versus mouse) to allow comparison of dietary approach independent of net caloric restriction. Clinically, we predominantly aimed to evaluate the safety, acceptability, and tolerability of each intervention, and obtained exploratory insight into changes in circulating markers, height-adjusted TKV (htTKV), and abdominal adiposity. We further evaluated health-related measures and PKD outcome efficacy of the different dietary intake regimens in the murine model. Together, these two studies elegantly and translationally delineate the feasibility of implementing dietary interventions as novel therapies for ADPKD patients and suggest that therapeutic benefit may be driven by changes in body weight rather than timing of caloric intake.

RESULTS

Human study

Enrollment and baseline clinical characteristics

One hundred twenty-two potential participants were pre-screened to assess initial eligibility (Figure S1). Major inclusion/exclusion criteria were: 18–65 years of age with ADPKD, baseline body mass index (BMI) of 25–45 kg/m^2, baseline CKD-EPI estimated glomerular filtration rate (eGFR) $\geq$30 mL/min/1.73m^2, non-diabetic, weight stable, and not participating in another weight loss program (complete criteria are described in the STAR Methods). Of these, 93 were excluded due to not meeting inclusion/exclusion criteria (n = 63) or declining to participate (n = 30). The most common reason for not meeting inclusion/exclusion criteria was that eGFR was too low (n = 38), followed by BMI being too low (n = 22). Twenty-nine participants were subsequently consented and screened for participation. One participant dropped after enrollment but prior to randomization (changed mind). Twenty-eight participants were randomized to a behavioral weight loss intervention based on either DCR or IMF. Two participants in the DCR group and one participant in the IMF group discontinued the intervention prior to month 3 for reasons unrelated to tolerability (DCR: moved out of the country, schedule conflicts; IMF: other life events/pandemic) and one participant in the IMF group discontinued prior to month 3 due to diet tolerability. Two participants in the DCR group discontinued the intervention prior to month 12 but were included in the analysis for data collected at month 3 (one dropped due to poor phone service/pandemic, one was lost to follow-up). One participant in the DCR group and one participant in the IMF group were not included in the MRI analysis due to contraindication (DCR) and not returning in person at 12 months due to COVID-19 (IMF), respectively. Characteristics of the 28 randomized participants are presented in Table 1. Of note, tolvaptan was not exclusionary; however, none of the participants were using tolvaptan at baseline or throughout the study.

Feasibility, safety, acceptability, and tolerability

The mean $\pm$ SD daily calorie goal in the DCR group was 1773 $\pm$ 253 kcals/day and the fast day calorie goal (3 days/week) in the IMF group was 532 $\pm$ 73 kcals/fasting day. On average, both groups achieved clinically significant (>5%) weight loss at month 3 (DCR: -7.1 ± 4.2%; IMF: -5.5 ± 3.3%, Figure 1A). At 12 months, participants in the DCR group had lost additional weight (-9.1 ± 6.0%) while weight loss in the IMF group plateaued (-4.9 ± 5.6%; $p < 0.05$ versus DCR at 12 months). Consistent with greater weight loss, self-reported dietary adherence (adherence score, 10 = perfect adherence) was better at 12 months in the DCR group: DCR 7.5 $\pm$ 0.67, IMF: 4.5 $\pm$ 0.84; $p < 0.05$ (Table S1). Further, DCR had more favorable safety and tolerability than IMF. Treatment-emergent adverse events related or possibly related to the intervention are shown in Table 2 among all participants and among participants who dropped out of the study in Table S2. Participants in the IMF group were more likely to experience hunger, fatigue, cold intolerance, irritability, and insomnia. One participant in the IMF group experienced adverse events (hunger, impaired concentration, cognitive difficulties, and lightheadedness) that resulted in a per protocol increase in the caloric intake goal on fasting days. The participant eventually dropped out of the study due to tolerability.

Compliance data and other questionnaires are presented in Table S1. Quality of life, mood, and physical activity did not significantly change over the duration of the intervention in either group. No participants met the Questionnaire on Eating and Weight Patterns-Revised (QEWP5) binge eating disorder screening criteria at any time point. Although visit attendance was similar in each group, self-reported dietary

Table 1. Baseline characteristics of study participants

Variable	Daily caloric restriction (n = 15)	Intermittent fasting (n = 13)	All participants (n = 28)
Age, y	47 ± 12	46 ± 6	46 ± 9
Sex, n (%) male	6 (40%)	6 (46%)	12 (43%)
Race/ethnicity, n (%) non-Hispanic white	13 (87%)	11 (85%)	24 (86%)
Weight, kg	103.3 ± 15.7	97.7 ± 10.7	100.7 ± 13.7
BMI, kg/m^2	34.6 ± 5.1	34.8 ± 5.1	34.7 ± 5.0
Waist circumference, cm	113.9 ± 10.6	109.5 ± 7.6	111.9 ± 9.4
Hip circumference, cm	118.5 ± 11.9	114.7 ± 13.0	116.7 ± 12.3
Waist to hip ratio	0.97 ± 0.12	0.96 ± 0.09	0.97 ± 0.11
SBP, mmHg	116 ± 12	125 ± 12	120 ± 13
DBP, mmHg	76 ± 8	84 ± 9	80 ± 9
CKD-EPI eGFR, mL/min/1.73m^2	64 ± 26	75 ± 16	69 ± 22
Fasting glucose, mg/dL	97 ± 12	92 ± 10	95 ± 11
Hypertension, n (%)	10 (67%)	10 (77%)	20 (71%)
ACEi/ARB, n (%)	12 (80%)	7 (54%)	19 (68%)
Statin, n (%)	3 (20%)	4 (31%)	7 (25%)
htTKV, mL/m	994 (589, 1,180)	835 (476, 1,363)	916 (476, 1,363)
Mayo class			
1A	1 (7%)	2 (15%)	3 (11%)
1B	3 (20%)	2 (15%)	5 (18%)
1C	5 (33%)	5 (39%)	10 (36%)
1D	2 (13%)	2 (15%)	4 (14%)
1E	2 (13%)	2 (15%)	4 (14%)
NA	2 (13%)	0 (0%)	0 (0%)

Data are mean ± S.D.or %. Height-adjusted total kidney volume (htTKV) and Mayo class missing in n = 2 in daily caloric restriction group due to contraindications. One participant with a contraindication in the IMF group subsequently dropped out of the study.

BMI, bodymass index; SBP, systolic blood pressure; DBP, diastolic blood pressure, CKD-EPI eGFR, estimated glomerular filtration rate by the Chronic Kidney Disease Epidemiology Collaboration equation; ACEi, angiotensin converting enzyme inhibitor; ARB, angiotensin receptor blocker.

adherence, difficulty to adhere, and likelihood to continue to adhere were all more favorable in the DCR group. The most frequently reported barriers to adherence are shown in Table S1.

Changes in anthropometrics, vital signs, and clinical labs are shown in Tables S3 and S4. Triglycerides, total cholesterol, and low-density lipoprotein cholesterol were only reduced in the DCR group ($p < 0.05$ at 12 months). Neither group demonstrated a change in eGFR, although percent change in weight was inversely correlated with change in eGFR in the DCR group ($r = -0.63$, $p = 0.04$).

Circulating and PBMC markers

Changes in circulating markers are shown in Tables S3 and S4. Insulin-like growth factor 1-binding protein (IGF1-BP), the ratio of IGF1 to IGF1-BP, leptin, interleukin-18 (IL-18), insulin, and hemostatic model assessment of insulin resistance (HOMA-IR) were only significantly reduced in the DCR group at 12 months ($p \leq 0.05$). Insulin and HOMA-IR differentially changed with DCR versus IMF ($p < 0.01$ for group*time interaction). C-reactive protein (CRP) was only reduced in the IMF group at 12 months ($p \leq 0.05$). The ratio of peripheral blood mononuclear cell (PBMC) protein expression of phosphorylated AMP-activated protein

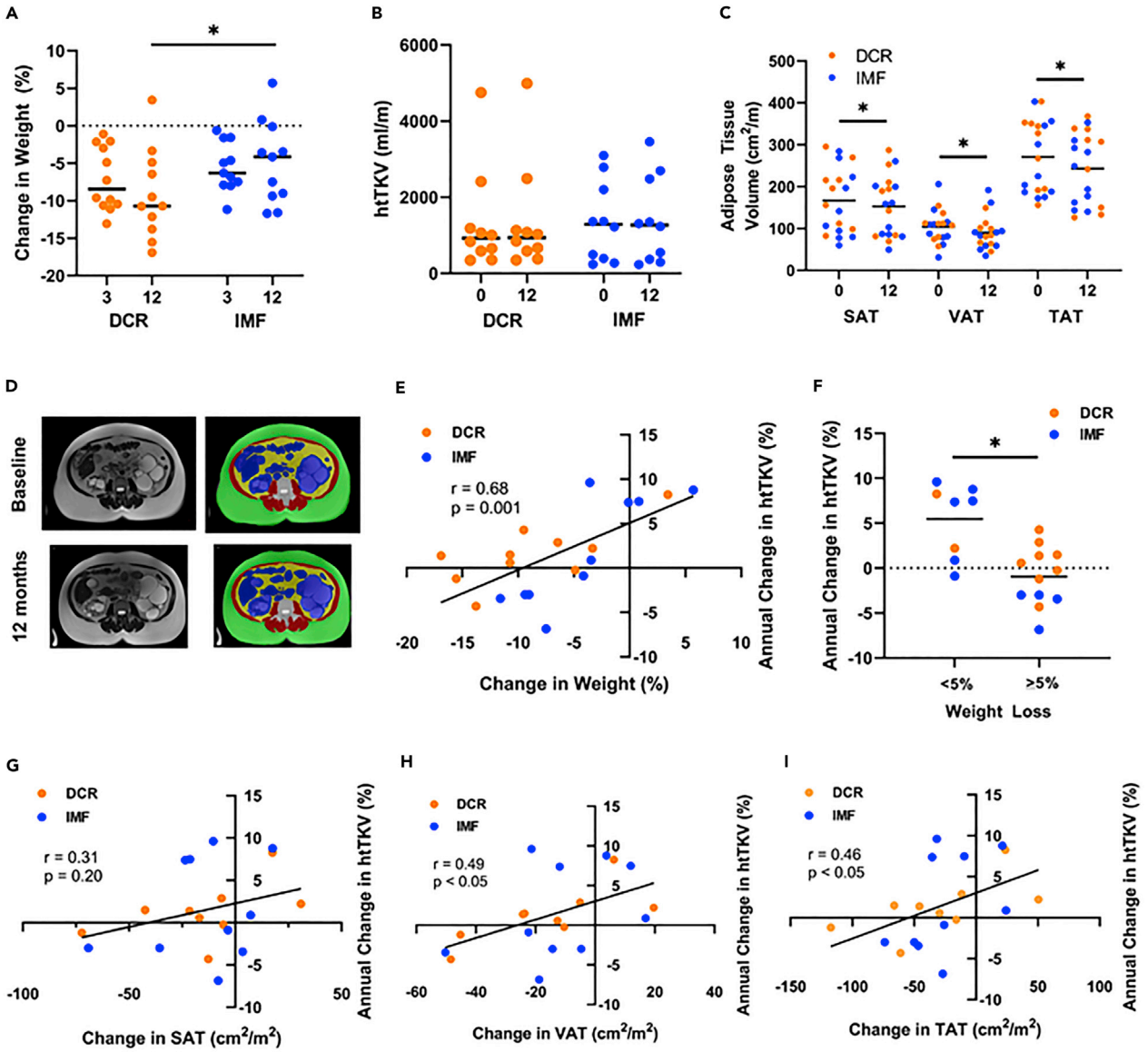

Figure 1. Weight loss with daily caloric restriction and intermittent fasting and association with kidney growth

(A) Percent weight loss according to group randomization (daily caloric restriction, DCR [orange], or intermittent fasting, IMF [blue]) at 3 months and 12 months; lines represent means with individual participants shown by dots. Clinically significant weight loss (>5%) was achieved in both groups at month 3. At 12 months, the DCR group lost additional weight, whereas weight loss in the IMF group plateaued.

(B) Height-adjusted total kidney volume (htTKV) according to group randomization (DCR or IMF) at baseline (0 months) and 12 months (lines represent median with individual participants shown by dots).

(C) Subcutaneous (SAT), visceral (VAT), and total adipose tissue (TAT) volume measured by abdominal MRI at baseline (0 months) and 12 months in pooled groups (lines represent mean with individual participants shown by dots). SAT, VAT, and TAT were all significantly reduced at 12 months.

(D) Representative MRI image of a DCR participant, with muscle in red (baseline: 87 cm^2/m; 12 months: 84 cm^2/m), SAT in green (baseline: 296 cm^2/m; 12 months: 253 cm^2/m), visceral organ in blue (baseline: 155 cm^2/m; 12 months: 162 cm^2/m), VAT in yellow (baseline: 108 cm^2/m; 12 months: 84 cm^2/m), and bone in white (baseline: 24 cm^2/m; 12 months: 23 cm^2/m).

(E and G–I) Association of percent change in weight (E), change in SAT (G), VAT (H), and TAT (I) at 12 months with annual percent change in htTKV. Among all participants, annual change in htTKV was correlated with change in weight, VAT, and TAT, but not SAT.

(F) When participants were categorized as losing clinically significant weight (≥5%; n = 12) at 12 months or not achieving this goal (n = 8), annual percent change in htTKV was significantly lower in the former group (Panel F). Statistics: Mixed effects model in repeated measures (panels A and B), paired t test (panel C), independent samples t test (panel F) and Pearson's bivariate correlation (panels E, G-I). P *<0.05 for group × time interaction based on a mixed effects model in repeated measures for weight at 12 months or t test.

Table 2. Adverse events related or possibly related to the intervention

Treatment-emergent adverse events	Daily caloric restriction (n = 15)	Intermittent fasting (n = 13)
Hunger	5 (33%)	11 (85%) *
Gastrointestinal distress (abdominal discomfort, constipation, nausea, or diarrhea)	4 (27%)	8 (62%)
Fatigue	1 (7%)	8 (62%) *
Lightheadedness/dizziness	3 (20%)	5 (39%)
Cold intolerance	1 (7%)	7 (54%) *
Change in mood	2 (14%)	4 (31%)
Irritability	1 (7%)	6 (46%) *
Insomnia	2 (13%)	7 (54%) *
Headache	2 (13%)	4 (31%)
Impaired concentration and/or cognitive difficulties	0 (0%)	3 (23%)
Tremor	0 (0%)	1 (8%)

Data are n (%). *p < 0.05 vs. daily caloric restriction by Fisher's exact test.

kinase (p-AMPK) to AMPK (p-AMPK/AMPK), but not the ratio of PBMC expression of phosphorylated S6 kinase (S6K) to S6K, differentially changed between groups at 12 months ($p < 0.05$ for group*time interaction, Figures 3A and 3C). Across both groups, p-AMPK/AMPK was correlated with annual percent change in htTKV ($r = -0.53$, $p < 0.05$, Figure 3C).

Magnetic resonance imaging

Given the pilot design of this clinical trial, annual change in htTKV was considered an exploratory endpoint and our *a priori* analysis plan was to present changes in htTKV as compared to historical data. Based on previous preclinical data indicating that food restriction slows cyst growth (Kipp et al., 2016; Warner et al., 2016), we predicted a slower annual percent change in htTKV with DCR compared to historic controls. Further, we expected a similar or greater result in the IMF group given that periods of fasting have been predicted to correct metabolic reprogramming (Boletta, 2016). Changes in abdominal MRI parameters, including htTKV, cyst volume, cystic index, abdominal adiposity and other abdominal compartments, are shown in Table 3, with htTKV and abdominal adiposity at baseline and 12 months shown graphically in Figures 1B and 1C. With data pooled across both groups, affording greater power, abdominal subcutaneous adipose tissue (SAT), visceral adipose tissue (VAT) and total adipose tissue (TAT) quantified by MRI were all significantly reduced at 12 months (Table 3 and Figure 1C). These measurements were obtained by adapting a methodology to quantify abdominal adiposity by computed tomography (CT) to differentiate SAT, muscle, VAT, visceral organ, and bone compartments using T2-weighted MRIs, as shown in a representative image in Figure 1D. A comparison of annual kidney growth and participant characteristics to several of the largest ADPKD cohorts (observational and interventional) is shown in Table S5, in accordance with our *a priori* statistical plan. Although the number of participants in the current study is small, and annual change in htTKV was an exploratory endpoint, the annual percent change in htTKV (DCR: $1.5 \pm 3.4\%$; IMF: $1.7 \pm 6.1\%$) is qualitatively low in comparison to historical data, despite relatively comparable, although not identical clinical characteristics. Notably, annual percent change in htTKV was highly correlated with percent change in weight ($r = 0.68$, $p = 0.001$, Figure 1E) and change in BMI at 12 months ($r = 0.63$, $p < 0.01$). When participants were categorized as either losing clinically significant body weight ($\geq 5\%$) at 12 months or not achieving this target, annual percent change in htTKV was significantly lower in the former group ($-1.0 \pm 3.3\%$ vs. $5.5 \pm 4.1\%$, $p < 0.01$, Figure 1F). Change in VAT ($r = 0.49$, $p < 0.05$) and TAT ($r = 0.46$, $p < 0.05$), but not SAT, also correlated with annual percent change in htTKV (Figures 1G–1I).

Animal study

DCR but not TRF or IMF associates with body weight loss in an orthologous mouse model of ADPKD1

To complement the human study, evaluate the impact of dietary regimens on PKD progression in the setting of normal body weight, and to expand the dietary intervention protocols to also include TRF, we

Table 3. Abdominal MRI parameters

	Daily caloric restriction n = 10		Intermittent fasting n = 10		Both groups n = 20	
	Baseline	12 months	Baseline	12 months	Baseline	12 months
htTKV, mL/m	921 [589, 1,180]	937 [587, 1,127]	1,288 [394, 2,204]	1,269 [367, 2,480]	1,032 [442, 1,783]	1,054 [463, 1,915]
Annual %Δ htTKV	NA	1.5 ± 3.4	NA	1.7 ± 6.1	NA	1.6 ± 4.8
Height-corrected cyst volume, mL/m	704 [433, 940]	735 [437, 944] *	1,008 [171, 1,871]	1,019 [198, 2,237] *	891 [258, 1,486]	925 [300, 1,687] *
Cystic index, fraction	0.72 ± 0.18	0.76 ± 0.20	0.67 ± 0.29	0.70 ± 0.28	0.69 ± 0.24	0.73 ± 0.24 *
Abdominal SAT, cm^2/m^2	182.5 ± 75.6	168.1 ± 78.6	153.2 ± 83.7	138.9 ± 67.9	167.1 ± 79.1	152.7 ± 72.6 *
Abdominal VAT, cm^2/m^2	105.2 ± 30.4	89.2 ± 30.9	102.6 ± 48.1	91.5 ± 49.6	103.8 ± 39.6	90.4 ± 40.7 *
Abdominal TAT, cm^2/m^2	287.7 ± 88.2	257.3 ± 96.9	255.8 ± 87.3	230.4 ± 76.7 *	270.9 ± 86.8	243.1 ± 85.5 *
Abdominal muscle, cm^2/m^2	87.5 ± 14.4	81.4 ± 16.6 *	89.4 ± 14.6	86.1 ± 10.8	88.5 ± 14.1	83.9 ± 13.7 *
Abdominal visceral organ, cm^2/m^2	141.1 ± 35.5	146.1 ± 37.9	160.3 ± 52.9	158.3 ± 48.4	151.2 ± 45.4	152.5 ± 43.0
Abdominal bone, cm^2/m^2	19.9 ± 4.8	21.0 ± 4.8	19.1 ± 1.8	19.4 ± 2.4	19.5 ± 3.5	20.1 ± 3.7

*$p \leq 0.05$ vs. baseline by paired t test. Data are mean ± SD or median [IQR]. htTKV, height-corrected total kidney volume; SAT, subcutaneous adipose tissue; VAT, visceral adipose tissue; TAT, total adipose tissue.

utilized the C57Bl/6J homozygous p.R3277C (*Pkd1*$^{RC/RC}$) ADPKD mouse model (Hopp et al., 2012; Arroyo et al., 2021) which mimics the genetics and pathophysiology of the human disease. The study duration was from 3 months (mo) of age to 6mo of age. We analyzed food intake and measured body weight (BW) at 1, 2, 4, 8, and 12 weeks into the study (Figure S2). Throughout the study, DCR and IMF animals, on Monday (Mo), Wednesday (We), Friday (Fr), consumed close to the targeted caloric restriction (DCR: 65.47% of *ad libitum* [AL]; IMF: 19.62% of AL), but IMF animals significantly overate on their AL days (Tuesday [Tu], Thursday [Th], Saturday [Sa], Sunday [Su]: 160.62% of AL). TRF animals only marginally reduced their food intake compared to AL animals, even though they only had an 8h window for food consumption (92.13% of AL, Figure S2A). At the beginning of the study, there was no difference in BW between animals assigned to the various feeding regimens independent of sex (Figures S2C and S2E). Consistent with the observation that IMF animals overate on their "off" days and that animals on TRF only slightly reduced their food intake throughout the study, TRF and IMF animals gained BW similarly to animals on AL feeding independent of sex (ΔBW [BW at 6mo – BW at 3mo] AL: 3.30g ± 1.16g, TRF: 3.11g ± 0.50g, IMF: 2.83g ± 0.80g, Figures 2A and S2B–S2E). However, DCR animals lost significant BW throughout the study duration compared to all other groups, with the steepest decline in BW occurring during the initial two weeks of the study (DCR ΔBW −3.19g ± 1.14g, $p < 0.0001$, Figures 2A and S2B–S2E).

Long-term daily DCR results in adverse health risks in normal weight Pkd1$^{RC/RC}$ mice

To begin to understand potential adverse health risks of the tested dietary regimens in normal weight PKD mice, we measured changes in lean mass by QMR, end of study internal organ mass and femur length in all *Pkd1*$^{RC/RC}$ animals. A decrease in lean mass is known to be associated with multiple health complications such as decreased immunity, increased muscle weakness, pneumonia, etc. (Argiles et al., 2016), and femur length allows assessment of proper growth. Neither TRF nor IMF animals showed a difference in Δ lean mass (lean mass at 6mo–3mo) or femur length compared to animals on AL feeding (Figures 2B and 2C). However, animals on DCR showed a significant decline of lean mass (AL: 2.90% ± 1.16% vs. DCR: −3.36% ± 1.06%, $P < 0.001$), a significant reduction in spleen mass normalized to body weight (%spleen weight/body weight, AL: 0.0041% ± 0.00074% vs. DCR: 0.0025% ± 0.00043%, $P < 0.001$) and a significant reduction in femur length (AL: 15.21mm ± 0.35mm vs. DCR: 14.62mm ± 0.22mm, $P < 0.05$) suggesting that long-term (3mo) DCR associates with growth retardation and may promote health complications in normal weight, adult C567Bl/6J*Pkd1*$^{RC/RC}$ mice (Figures 2B, 2C, and S3A, Assessment of PKD-severity and associated pathologies/physiologies in the murine trial).

Direct comparison of therapeutic efficacy highlights DCR as the only dietary regimen to alleviate cystic kidney disease severity in ADPKD1 mice

To assess the therapeutic efficacy of the tested feeding regimens on alleviating PKD severity we evaluated kidney phenotypes classically analyzed in murine PKD studies. Gross histological examination of

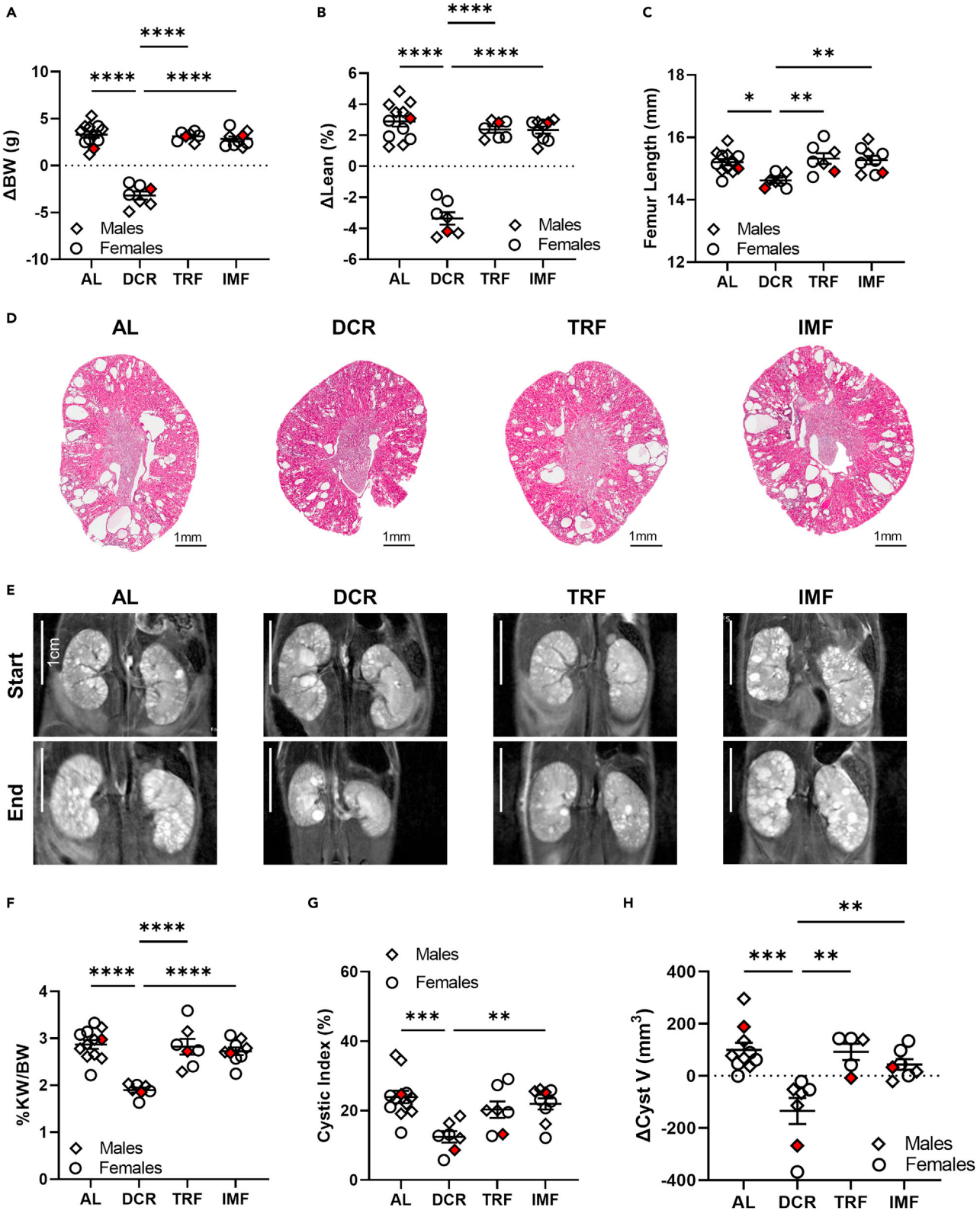
A
ΔBW (g)
Males
Females
AL
DCR
TRF
IMF
B
ΔLean (%)
C
Femur Length (mm)
D
AL
DCR
TRF
IMF
1mm
E
Start
End
1cm
F
%KW/BW
G
Cystic Index (%)
H
ΔCyst V (mm3)

Figure 2. Daily caloric restriction but not time restricted feeding or intermittent fasting alleviates PKD in an orthologous ADPKD mouse model

(A) Change in body weight from start of study (3 months [mo]) to end of study (6mo) of C57Bl/6J*Pkd1*$^{RC/RC}$ mice adhering to either *ad libitum* feeding (AL), daily caloric restriction (DCR), time restricted feeding (TRF), or intermittent fasting (IMF). Only animals on DCR lost weight throughout the duration of the study. Mice on TRF or IMF gained weight comparably to mice eating freely (AL).

(B) Percent change in lean mass as analyzed by quantitative magnetic resonance from start of study to end of study. Mice on DCR lost a significant amount of lean mass, while mice on AL, TRF, and IMF gained lean mass comparably.

(C) Femur length at end of study as measure of adequate growth. The femur length of mice on DCR was significantly shorter than the femur length of mice adhering to AL, TRF, or IMF suggesting that DCR impacts healthy growth.

(D) Representative H&E kidney cross sections.

(E) Representative magnetic resonance (MR) images at study start/end. The same animals are shown at start/end of study and as in (D).

(F) Percent kidney weight/body weight (%KW/BW) of all study animals measured at end of study.

(G) Cystic index (percent area cystic/total) as measured from three H&E cross sections per animal of all study animals.

(H) Change in cystic volume (cystic V study end – cystic V study start) as measured by MR imaging from all study animals. N: AL (8M, 4F), DCR (3M, 4F), TRF (3M, 4F), IMF (4F, 5M). Red data points indicate representative animals shown in (D) and (E). Mean ± SEM shown. Statistics: ANOVA with Tukey's post-hoc. P *<0.05, **<0.01, ***<0.001, ****<0.0001. See also Figures S2–S4.

H&E-stained kidney cross sections obtained at study end showed a marked decrease in cystic disease burden in animals on DCR compared to animals on AL, TRF, or IMF; the cystic phenotype of animals on AL, TRF, or IMF were indistinguishable from each other (Figure 2D). In line with that observation, percent kidney weight over body weight (%KW/BW) was only significantly decreased in animals on DCR compared to animals on AL, TRF, or IMF, with no significant differences when comparing mice on TRF or IMF to mice on AL feeding (%KW/BW DCR: 1.90 ± 0.15, AL: 2.87 ± 0.32, TRF: 2.82 ± 0.44, IMF: 2.73 ± 0.24; $P < 0.0001$, Figures 2F, S2C, and S2E). No differences in efficacy based on sex were noted. Since the normalizing variable, BW, was significantly impacted by our treatment design, we also normalized KW to heart weight, which was not significantly different among groups at study end (Figures S3A and S3B). Independent of the normalizing variable, it remained that only animals on DCR feeding had a significantly reduced kidney weight compared to animals on AL feeding.

The observed reduction in kidney weight of animals on DCR compared to animals on AL or the alternate feeding regimens coincided with a significant decrease in cystic index, cyst number, and cyst size (Figures 2G and S4A–S4C, Detailed analysis of kidney cystic burden across study groups within the murine trial). These findings were confirmed by our pre- and post-study MRI analyses. As previously shown, the cyst volume in animals on DCR declined throughout the study while cysts continued to grow in animals on AL, TRF, or IMF (Figures 2E and 2H) (Warner et al., 2016). This was also reflected in TKV, although the decline in TKV of animals on DCR versus AL did not reach statistical significance; the TKV of study animals at study-start was not significantly different between groups (Figures S2D and S2E). In line with therapeutic efficacy of DCR, kidney composition (cyst versus tissue) only changed in animals on DCR versus animals on AL, TRF or IMF, with kidney volume occupied by cysts decreasing significantly (Figure S2F).

Lastly, we evaluated kidney function via measurement of blood urea nitrogen (BUN) and kidney fibrotic burden. While BUN did not change independent of feeding regimen, computed fibrotic volume (fibrotic index adjusted for kidney size) significantly decreased in animals on DCR versus AL or the alternate feeding regimens (Figures S3C and S3D). The fact that DCR did not improve kidney function, although it showed efficacy to alleviate disease for all other analyzed parameters is not surprising, given that at 6mo of age C57Bl/6J*Pkd1*$^{RC/RC}$ animals have only marginally elevated BUN levels compared to wildtypes, which are nowhere close to levels considered typical for physiologically significant kidney function decline (>70mg/dL).

Different dietary intake regimens have a distinct impact on cellular pathways

To begin to elucidate signaling cascades that may contribute to the therapeutic efficacy of DCR versus TRF and IMF in alleviating PKD, we performed western blotting of proteins known to be impacted by these dietary regimens using whole kidney lysates. In contrast to prior publications, we did not see a reduction in p-S6/S6 levels in animals on DCR versus AL (Figure 3B) (Warner et al., 2016; Kipp et al., 2016). Kidneys of animals on DCR, however, showed a significant increase in p-AMPK/AMPK compared to animals on AL and TRF, and a trend toward increase compared to animals on IMF (Figures 3B and 3D). Since reduced levels of p-AMPK/AMPK are hallmark of PKD progression, correction of this dysregulation is in line with the observed therapeutic effect seen in animals on DCR. We also assayed autophagy markers (LC3-II/LC3-I ratio [autophagosome formation] and p62 [autophagosome cargo protein]), p-LKB1/LKB1 ratio, and SIRT1, but the levels of these proteins were not altered in any of the dietary regimens compared to AL (Figure 3B).

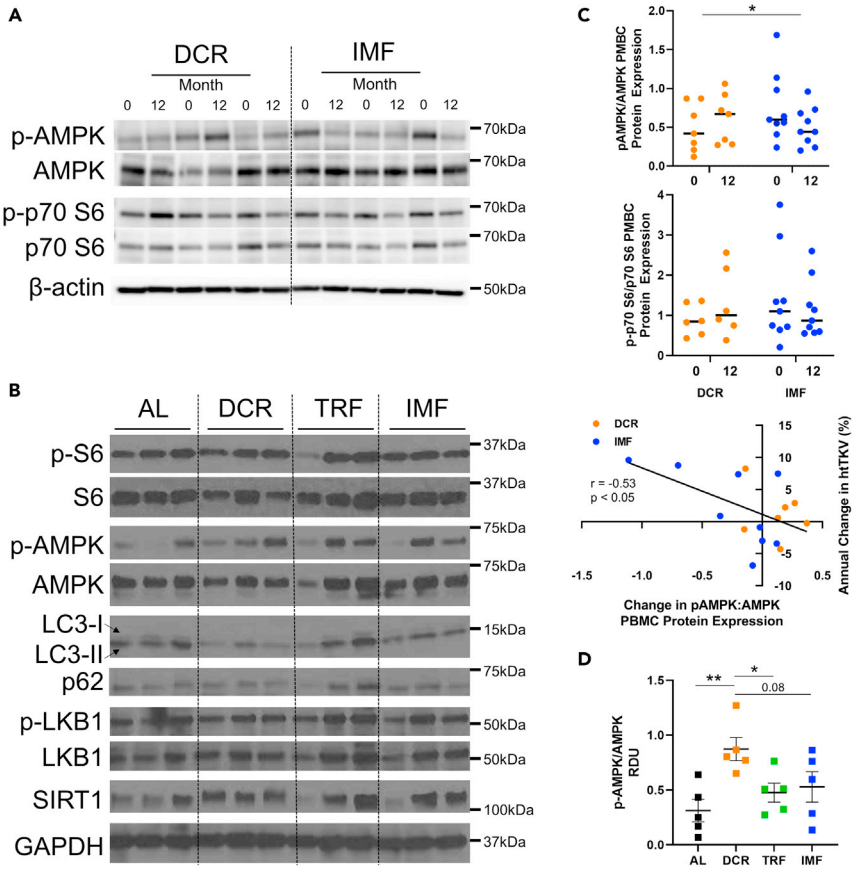

Figure 3. Cellular changes in human PBMCs and mouse kidneys are distinct among dietary regimens

(A and B) Representative Western blot images of (A) Peripheral blood mononuclear cells (PBMCs) from three humans/group, pre- and post-treatment and (B) whole kidney homogenates from three mice per dietary regimen.

(C) Quantification of human Western blot (A), N: 6–9/group. The ratio of PBMC phosphorylated-AMP-activated kinase (p-AMPK) to AMPK (p-AMPK/AMPK), but not the ratio of phosphorylated p70 S6 kinase (p-p70 S6) to p70 S6 (p-p70 S6/S6) changed between daily caloric restriction (DCR) and intermittent fasting (IMF) groups. Mean ± SEM shown. RDU: relative density unit, normalized to β-actin levels. Statistics: independent samples t test comparing change between groups. P *<0.05.

(D) Quantification of mice Western blot (B), N: 5mice/group, both females and males. Animals on DCR show a significant increase in p-AMPK/AMPK levels. Quantification for ratios of p-S6/S6, p-LKB1/LKB1, LC3-II/LC3-I (arrows), and levels of p62 as well as SIRT1 showed no significant differences between groups (data not shown). AL: *ad libitum*, TRF: time restricted feeding. Mean ± SEM shown. RDU: relative density unit, normalized to GAPDH levels. Statistics: unpaired t test. P *<0.05, **<0.01.

DISCUSSION

We have performed the first clinical trial of behavioral weight loss though DCR or IMF in humans with ADPKD. Foremost, our year-long study supports the feasibility and tolerability of DCR in particular. Difficulties with tolerability and adherence in the IMF group highlight that DCR may be a more feasible dietary intervention in adults with ADPKD. We were also able to gather exploratory evidence that suggests weight loss may slow kidney growth in overweight and obese adults with ADPKD independent of the dietary regimen implemented. Our human study was designed as a weight loss intervention based on our prior epidemiological observation that ADPKD progression is substantially faster with higher BMI (Nowak et al., 2018). Our primary goal was to determine the feasibility of a behavioral weight loss intervention based on DCR or IMF in adults with ADPKD and overweight or obesity. Recognizing that annual change in htTKV was an exploratory endpoint to help power a future larger trial, we expected that the IMF group would show a trend toward greater benefit than the DCR group due to metabolic reprogramming associated with periodic fasting (Boletta, 2016) in addition to weight loss observed in non-ADPKD IMF

intervention studies (Catenacci et al., 2016; Trepanowski et al., 2017). In contrast, we observed a similar annual kidney growth in both groups that was qualitatively low compared to historical controls, and on average, a cessation of kidney growth in participants who achieved clinically significant weight loss. Interestingly, we further observed a correlation between weight loss, reduced abdominal adiposity, and slower kidney growth. These findings, corroborated by our epidemiological observations (Nowak et al., 2018, 2021) and our preclinical observation suggest that weight loss may be an important therapeutic player of the beneficial effects of caloric restriction to slow cyst growth in ADPKD. However, metabolic reprogramming due to lower overall caloric intake and/or periods of fasting, could also be a key mechanistic driver of the therapeutic efficacy observed in our study, with weight loss (which, by definition, is also associated with metabolic reprogramming) occurring secondarily.

Our human study was complemented by a parallel direct comparison of the three most widely accepted feeding regimens (DCR, IMF, and TRF) in an orthologous ADPKD1 mouse model. This was the first evaluation of IMF in a murine PKD model and the first long-term study of TRF in an orthologous murine ADPKD model. In our mouse model, only DCR was efficacious in slowing cystic kidney disease progression, an observation described previously (Warner et al., 2016; Kipp et al., 2016). In contrast, the lack of benefit with TRF is not in line with a recent publication, which studied TRF in the Han:SPRD rat model (Torres et al., 2019). This may be explained by a difference in (1) the driving PKD gene (*Anks6*, Han:SPRD rat versus *Pkd1*, $Pkd1^{RC/RC}$ mouse), (2) the timing of disease progression (rapid versus slow), (3) the pathophysiology between species and/or background, or (4) the intervention duration (5 weeks, Han:SPRD rat, versus 3 months, $Pkd1^{RC/RC}$ mouse). The lack of therapeutic effect in animals on IMF may be attributed to IMF animals compensating by overeating on non-fasting days, which differs from humans with an above ideal BMI, who adjust to a new set point (Klempel et al., 2010). However, future studies will be focused on delineating potential mechanisms unique to DCR or weight loss that attribute to the therapeutic effect we observed in the $Pkd1^{RC/RC}$ mouse. Of note, our preclinical observations are consistent with our human data and suggest that fasting alone without weight loss may not have beneficial effects on slowing ADPKD progression. Notably, even though our study animals in the IMF or TRF group did not achieve weight loss as predicted, they nonetheless successfully completed a caloric intake fasting regimen per protocol definition.

In our human study, feasibility, tolerability, and acceptability were all more favorable in the DCR group. While weight loss was clinically significant in both groups, weight loss plateaued after 3 months in the IMF group, but it continued in the DCR group through the end of the study. The overall level of weight loss in the DCR group (9%) was quite high, notable given virtual intervention delivery, which has shown more limited benefit in the general population (Sorgente et al., 2017). Importantly, all participants received regular behavioral support in a structured group setting with instruction by a well-qualified registered dietician, which may differ from a real-world setting.

A novel exploratory aspect of our human study was the assessment of abdominal adiposity by MRI. Our results suggest that reductions in adipose tissue, likely visceral, may be implicated in the beneficial effects of weight loss. Recognizing that unlike our human trial, our PKD model used is not a model of obesity, and it is interesting to note that the therapeutic effect was only observed in animals that adhered to a dietary regimen resulting in weight loss. This suggests that, as in our clinical study, body weight may be the key modifier of PKD progression. It is important to note that both the DCR study using the rapidly progressive mosaic mouse model (23% reduction in daily caloric intake) (Kipp et al., 2016) and the TRF study in the Han:SPRD rat model (Torres et al., 2019) achieved efficacy in slowing PKD without an overall change in BW with treatment versus control. Again, model choice or timing of disease progression may explain the discrepant results. In the prior orthologous $Pkd1^{RC/RC}$ model study, even 10% DCR from *ad libitum* resulted in decreased BW, thus, making it impossible to determine the underlying driver of efficacy (Warner et al., 2016). This nuance is critical to acknowledge when designing/evaluating future preclinical trials in PKD. If weight loss occurs in the treatment arm, treatment efficacy needs to be evaluated cautiously. It is also important to acknowledge potential adverse health effects of DCR in normal weight mice, as reflected by reduced lean mass, spleen mass, and femur length. Notably, growing, non-obese mice differ physiologically from overweight and obese adults. Thus, while loss of body weight may be beneficial in humans with above normal BMI, individuals already of ideal body weight may require caution when considering weight loss regimens. This consideration is consistent with data from the 2-year multi-center randomized controlled trial CALERIE (Comprehensive Assessment of Long-Term Effects of Reducing Intake of Energy),

which observed that 25% DCR in healthy non-obese adults was associated with potential risk of bone loss and anemia (Romashkan et al., 2016).

By design, we are limited in the ability to discern specific mechanistic insight. We did observe an increase in p-AMPK with DCR both in whole kidney lysate from mice and human PBMCs. We acknowledge that kidney expression was not location specific, that it was not possible to analyze kidney tissue from humans, and that we were limited in the number of PBMC proteins we could analyze. Consistent with the literature, we observed an increase in p-AMPK/AMPK without changes to autophagy with DCR; however, we did not observe changes to p-LKB1/LKB1 or p-S6/S6 (mouse and human) ratios as have been previously reported with dietary regiments in rodents (Warner et al., 2016; Torres et al., 2019; Kipp et al., 2016). The underlying reason for this requires further investigation.

The major strength of this study is our translational study design incorporating complementary human and animal data, including assurance of feasibility in this first dietary restriction and weight loss trial in humans with ADPKD. We provided measures of abdominal adiposity using MRI images collected to measure TKV and a rigorously designed intervention administered by registered dieticians. In our mouse study, we performed the first assessment of IMF in a PKD model, the first study of TRF in an orthologous ADPKD model, and a direct comparison of three different dietary regimens. The animals were individually housed with gated food hoppers for precise regulation of feeding times and amounts.

Limitations of the study

Due to lack of prior data, the human study was designed as a pilot and feasibility study; thus, the sample size is small, htTKV data while an *a priori* endpoint were exploratory, and a control group was not included. Given that the primary outcome of this pilot study was feasibility, two active groups were determined to be a more valuable design than including a control group. We concluded that DCR was a more feasible intervention than IMF, which was the primary goal of the pilot study. We did not include a TRF group in this human study; a pilot study evaluating the feasibility of TRF in adults with ADPKD and overweight/obesity is ongoing (NCT04534985). We were unable to assess β-hydroxybutyrate due to lack of stability in stored samples and COVID-19 associated limitations in obtaining fresh samples. However, loss of body fat as observed in our human study is directly linked with induction of ketosis (Goss et al., 2020). Of note, the recent study on ketosis in the Han:SPRD rat (Torres et al., 2019) was published after our studies were well underway. In contrast to the human study, the mouse model was not a model of obesity; development of such an ADPKD mouse model would be an interesting future direction. Statistical testing was not adjusted for multiple comparisons given the exploratory nature of many outcomes in the human study; thus, significant p values may be spurious. Last, the mechanisms of beneficial effects of DCR need to be further delineated, to understand whether changes are occurring at the gene, protein and/or metabolite level, and to elucidate why DCR but not TRF/IMF may work in the *Pkd1*$^{RC/RC}$ mouse model.

A key future direction is determining which (metabolic) pathway is the key modulator of the beneficial effects of DCR and/or weight loss. This would facilitate subsequent research on pharmaceutical alternatives, i.e., DCR mimetics. It would also be highly clinically significant to establish visceral or total adiposity as a novel biomarker of disease progression. It is worth highlighting that lifestyle interventions have great potential for clinical impact on ADPKD, which slowly progresses across a lifetime. Weight loss via DCR can be combined with tolvaptan (or other therapies); we recently reported similar efficacy of tolvaptan irrespective of BMI (Nowak et al., 2021). A larger phase 2 trial with a direct comparison of DCR to a control group, powered for a primary endpoint of change in htTKV, will be starting this year (NCT04907799). Our results also have implications for individuals who are not overweight or obese as well as those who achieve an ideal BMI via weight loss, as they underscore the importance of maintaining a normal BMI as a potential specific strategy to slow the trajectory of their ADPKD progression.

STAR★METHODS

Detailed methods are provided in the online version of this paper and include the following:

- KEY RESOURCES TABLE
- RESOURCE AVAILABILITY
  - Lead contact

SUPPLEMENTAL INFORMATION

Supplemental information can be found online at https://doi.org/10.1016/j.isci.2021.103697.

ACKNOWLEDGMENTS

This work was supported by the National Institutes of Health (NIH) National Institute of Diabetes and Digestive and Kidney Diseases (NIDDK) R03DK118215, Colorado Clinical and Translational Sciences Institute Colorado Junior Faculty Award CO-J-18-37, NIH National Center for Advancing Translational Sciences (NCATS) Colorado Clinical and Translational Science Award UL1 TR002535, PKD Foundation Research Grant 241G20a, the University of Colorado Nutrition Obesity Research Center (NIDDK grant P30DK048520), the University of Colorado Cancer Center Animal Imaging Shared resource (P30CA046934), and NIH high-end instrumentation grant S10OD018435. Kristen Nowak is also supported by K01DK103678 and by the Baltimore PKD Research and Clinical Core Center Pilot and Feasibility Program (grant number P30DK090868). K.H. is also supported by K01DK114164 and DK114164-03S1. Cortney Steele is supported by NIDDK (grant 5T32DK007135-46). This work was also supported by the Zell family foundation. Contents are the authors' sole responsibility and do not necessarily represent official NIH or PKD Foundation views.

AUTHOR CONTRIBUTIONS

Conceptualization: K.H., V.C., M.C., K.L.N; Methodology: K.H., N.D., T.L.K., D.T.N., B.P., G.C.J., M.R.J., C.S., P.S.M., K.L.N.; Software: T.L.K.; Validation: K.H., N.D., W.W., K.L.N.; Formal Analysis: K.H., Z.Y., N.J.S., K.L.N.; Investigation: K.H., V.C., N.D., T.L.K., W.W., K.B., B.P., M.M., C.S., B.G., M.C., K.L.N.; Resources: K.B., M.M; Writing – Original Draft: K.H., K.L.N.; Writing – Review & Editing: V.C., T.L.K., W.W., Z.Y., K.B., B.P., C.S., N.J.S., B.G., R.A.N., M.C.; Visualization: K.H., K.L.N.; Supervision: M.C., V.C.; Funding Acquisition: K.H., R.A.N., B.G., M.C, K.L.N.

DECLARATION OF INTERESTS

K.H. receives royalties for industry use of the *Pkd1*$^{RC/RC}$ mouse model in concordance with Mayo Clinic Ventures regulations (Mayo Technology Case #2012–14). B.G. is a member of the PKD Foundation Scientific Advisory Committee.

INCLUSION AND DIVERSITY

We worked to ensure gender balance in the recruitment of human subjects. We worked to ensure ethnic or other types of diversity in the recruitment of human subjects. We worked to ensure sex balance in the selection of non-human subjects. One or more of the authors of this paper self-identifies as an underrepresented ethnic minority in science.

Received: October 6, 2021
Revised: November 19, 2021
Accepted: December 21, 2021
Published: January 21, 2022

SUPPORTING CITATIONS

The following reference appears in the Supplemental information: Chapman et al., 2012; Irazabal et al., 2016; Irazabal et al., 2017; Meijer et al., 2018; Schrier et al., 2014; Torres et al., 2012.

REFERENCES

Argiles, J.M., Campos, N., Lopez-Pedrosa, J.M., Rueda, R., and Rodriguez-Manas, L. (2016). Skeletal muscle regulates metabolism via interorgan crosstalk: roles in health and disease. J. Am. Med. Dir. Assoc. *17*, 789–796. https://doi.org/10.1016/j.jamda.2016.04.019.

Arroyo, J., Escobar-Zarate, D., Wells, H.H., Constans, M.M., Thao, K., Smith, J.M., Sieben, C.J., Martell, M.R., Kline, T.L., Irazabal, M.V., et al. (2021). The genetic background significantly impacts the severity of kidney cystic disease in the pkd1(rc/rc) mouse model of autosomal dominant polycystic kidney disease. Kidney Int. *99*, 1392–1407. https://doi.org/10.1016/j.kint.2021.01.028.

Beck, A.T., Steer, R.A., and Garbin, G.M. (1988). Psychometric properties of the beck depression inventory: twenty-five years of evaluation. Clin. Psychol. Rev. *8*, 77–100.

Boletta, A. (2016). Slowing polycystic kidney disease by fasting. J. Am. Soc. Nephrol. *27*, 1268–1270. https://doi.org/10.1681/ASN.2015101113.

Brunt, V.E., Wiedenfeld-Needham, K., Comrada, L.N., and Minson, C.T. (2018). Passive heat therapy protects against endothelial cell hypoxia-reoxygenation via effects of elevations in temperature and circulating factors. J. Physiol. *596*, 4831–4845. https://doi.org/10.1113/JP276559.

Catenacci, V.A., Pan, Z., Ostendorf, D., Brannon, S., Gozansky, W.S., Mattson, M.P., Martin, B., Maclean, P.S., Melanson, E.L., and Troy Donahoo, W. (2016). A randomized pilot study comparing zero-calorie alternate-day fasting to daily caloric restriction in adults with obesity. Obesity *24*, 1874–1883. https://doi.org/10.1002/oby.21581.

Chapman, A.B., Guay-Woodford, L.M., Grantham, J.J., Torres, V.E., Bae, K.T., Baumgarten, D.A., Kenney, P.J., King, B.F., Jr., Glockner, J.F., Wetzel, L.H., et al. (2003). Renal structure in early autosomal-dominant polycystic kidney disease (ADPKD): the consortium for radiologic imaging studies of polycystic kidney disease (CRISP) cohort. Kidney Int. *64*, 1035–1045. https://doi.org/10.1046/j.1523-1755.2003.00185.x.

Chapman, A.B., Bost, J.E., Torres, V.E., Guay-Woodford, L., Bae, K.T., Landsittel, D., Li, J., King, B.F., Martin, D., Wetzel, L.H., et al. (2012). Kidney volume and functional outcomes in autosomal dominant polycystic kidney disease. Clin. J. Am. Soc. Nephrol. *7*, 479–486. https://doi.org/10.2215/CJN.09500911.

Dansinger, M.L., Gleason, J.A., Griffith, J.L., Selker, H.P., and Schaefer, E.J. (2005). Comparison of the atkins, ornish, weight watchers, and zone diets for weight loss and heart disease risk reduction: a randomized trial. JAMA *293*, 43–53. https://doi.org/10.1001/jama.293.1.43.

De Kreutzenberg, S.V., Ceolotto, G., Cattelan, A., Pagnin, E., Mazzucato, M., Garagnani, P., Borelli, V., Bacalini, M.G., Franceschi, C., Fadini, G.P., et al. (2015). Metformin improves putative longevity effectors in peripheral mononuclear cells from subjects with prediabetes. A randomized controlled trial. Nutr.Metab.Cardiovasc. Dis. *25*, 686–693. https://doi.org/10.1016/j.numecd.2015.03.007.

Garner, D.M., Olmsted, M.P., Bohr, Y., and Garfinkel, P.E. (1982). The eating attitudes test: psychometric features and clinical correlates. Psychol. Med. *12*, 871–878. https://doi.org/10.1017/s0033291700049163.

Goss, A.M., Gower, B., Soleymani, T., Stewart, M., Pendergrass, M., Lockhart, M., Krantz, O., Dowla, S., Bush, N., Garr Barry, V., et al. (2020). Effects of weight loss during a very low carbohydrate diet on specific adipose tissue depots and insulin sensitivity in older adults with obesity: a randomized clinical trial. Nutr.Metab. *17*, 64. https://doi.org/10.1186/s12986-020-00481-9.

Grantham, J.J., Torres, V.E., Chapman, A.B., Guay-Woodford, L.M., Bae, K.T., King, B.F., Jr., Wetzel, L.H., Baumgarten, D.A., Kenney, P.J., Harris, P.C., et al. (2006). Volume progression in polycystic kidney disease. N. Engl. J. Med. *354*, 2122–2130. https://doi.org/10.1056/NEJMoa054341.

Grunwald, G.K., Melanson, E.L., Forster, J.E., Seagle, H.M., Sharp, T.A., and Hill, J.O. (2003). Comparison of methods for achieving 24-hour energy balance in a whole-room indirect calorimeter. Obes. Res. *11*, 752–759. https://doi.org/10.1038/oby.2003.105.

Hays, R.D., and Morales, L.S. (2001). The RAND-36 measure of health-related quality of life. Ann. Med. *33*, 350–357.

Helal, I., Mcfann, K., Reed, B., Yan, X.D., and Schrier, R.W. (2013). Changing referral characteristics of patients with autosomal dominant polycystic kidney disease. Am. J. Med. *126*, 832.e11. https://doi.org/10.1016/j.amjmed.2012.12.018.

Hoddy, K.K., Kroeger, C.M., Trepanowski, J.F., Barnosky, A., Bhutani, S., and Varady, K.A. (2014). Meal timing during alternate day fasting: impact on body weight and cardiovascular disease risk in obese adults. Obesity *22*, 2524–2531. https://doi.org/10.1002/oby.20909.

Hopp, K., Hommerding, C.J., Wang, X., Ye, H., Harris, P.C., and Torres, V.E. (2015). Tolvaptan plus pasireotide shows enhanced efficacy in a pkd1 model. J. Am. Soc. Nephrol. *26*, 39–47. https://doi.org/10.1681/ASN.2013121312.

Hopp, K., Ward, C.J., Hommerding, C.J., Nasr, S.H., Tuan, H.F., Gainullin, V.G., Rossetti, S., Torres, V.E., and Harris, P.C. (2012). Functional polycystin-1 dosage governs autosomal dominant polycystic kidney disease severity. J. Clin.Invest. *122*, 4257–4273. https://doi.org/10.1172/JCI64313.

Institute of Laboratory Animal Research (2011). Guide for the Care and Use of Laboratory Animals (National Academies Press).

Irazabal, M.V., Rangel, L.J., Bergstralh, E.J., Osborn, S.L., Harmon, A.J., Sundsbak, J.L., Bae, K.T., Chapman, A.B., Grantham, J.J., Mrug, M., et al. (2015). Imaging classification of autosomal dominant polycystic kidney disease: a simple model for selecting patients for clinical trials. J. Am. Soc. Nephrol. *26*, 160–172. https://doi.org/10.1681/ASN.2013101138.

Irazabal, M.V., Blais, J.D., Perrone, R.D., Gansevoort, R.T., Chapman, A.B., Devuyst, O., Higashihara, E., Harris, P.C., Zhou, W., Ouyang, J., et al. (2016). Prognostic enrichment design in clinical trials for autosomal dominant polycystic kidney disease: the TEMPO 3:4 clinical trial. Kidney Int. Rep. *1*, 213–220. https://doi.org/10.1016/j.ekir.2016.08.001.

Irazabal, M.V., Abebe, K.Z., Bae, K.T., Perrone, R.D., Chapman, A.B., Schrier, R.W., Yu, A.S., Braun, W.E., Steinman, T.I., Harris, P.C., et al. (2017). Prognostic enrichment design in clinical trials for autosomal dominant polycystic kidney disease: the HALT-PKD clinical trial. Nephrol.Dial.Transpl. *32*, 1857–1865. https://doi.org/10.1093/ndt/gfw294.

Johnson, J.B., Summer, W., Cutler, R.G., Martin, B., Hyun, D.H., Dixit, V.D., Pearson, M., Nassar, M., Telljohann, R., Maudsley, S., et al. (2007). Alternate day calorie restriction improves clinical findings and reduces markers of oxidative stress and inflammation in overweight adults with moderate asthma. Free Radic. Biol. Med. *42*, 665–674. https://doi.org/10.1016/j.freeradbiomed.2006.12.005.

Kipp, K.R., Rezaei, M., Lin, L., Dewey, E.C., and Weimbs, T. (2016). A mild reduction of food intake slows disease progression in an orthologous mouse model of polycystic kidney disease. Am. J. Physiol. Ren. Physiol *310*, F726–F731. https://doi.org/10.1152/ajprenal.00551.2015.

Kleczko, E.K., Marsh, K.H., Tyler, L.C., Furgeson, S.B., Bullock, B.L., Altmann, C.J., Miyazaki, M., Gitomer, B.Y., Harris, P.C., Weiser-Evans, M.C.M., et al. (2018). Cd8(+) t cells modulate autosomal dominant polycystic kidney disease progression. Kidney Int. *94*, 1127–1140. https://doi.org/10.1016/j.kint.2018.06.025.

Klempel, M.C., Bhutani, S., Fitzgibbon, M., Freels, S., and Varady, K.A. (2010). Dietary and physical activity adaptations to alternate day modified fasting: implications for optimal weight loss. Nutr.J. *9*, 35. https://doi.org/10.1186/1475-2891-9-35.

Kline, T.L., Edwards, M.E., Fetzer, J., Gregory, A.V., Anaam, D., Metzger, A.J., and Erickson, B.J. (2020). Automatic semantic segmentation of kidney cysts in mr images of patients affected by autosomal-dominant polycystic kidney disease. Abdom.Radiol. https://doi.org/10.1007/s00261-020-02748-4.

Kline, T.L., Edwards, M.E., Korfiatis, P., Akkus, Z., Torres, V.E., and Erickson, B.J. (2016). Semiautomated segmentation of polycystic kidneys in T2-weighted MR images. AJR Am. J. Roentgenol *207*, 605–613. https://doi.org/10.2214/AJR.15.15875.

Levey, A.S., Stevens, L.A., Schmid, C.H., Zhang, Y.L., Castro, A.F., 3rd, Feldman, H.I., Kusek, J.W., Eggers, P., Van Lente, F., Greene, T., et al. (2009). A new equation to estimate glomerular filtration rate. Ann. Intern. Med. *150*, 604–612.

Matthews, D.R., Hosker, J.P., Rudenski, A.S., Naylor, B.A., Treacher, D.F., and Turner, R.C. (1985). Homeostasis model assessment: insulin resistance and beta-cell function from fasting plasma glucose and insulin concentrations in man. Diabetologia *28*, 412–419.

Mcnair, D., Lorr, M., and Droppleman, L. (1971). Profile of Mood States (POMS) Manual (Education and Industrial Testing Service).

Meijer, E., Visser, F.W., Van Aerts, R.M.M., Blijdorp, C.J., Casteleijn, N.F., D'agnolo, H.M.A., Dekker, S.E.I., Drenth, J.P.H., De Fijter, J.W., Van Gastel, M.D.A., et al. (2018). Effect of lanreotide on kidney function in patients with autosomal dominant polycystic kidney disease: the DIPAK 1 randomized clinical trial. JAMA *320*, 2010–2019. https://doi.org/10.1001/jama.2018.15870.

Nangle, D.W., Johnson, W.G., Carr-Nangle, R.E., and Engler, L.B. (1994). Binge eating disorder and the proposed DSM-IV criteria: psychometric analysis of the questionnaire of eating and weight patterns. Int. J.Eat.Disord. *16*, 147–157.

Nowak, K.L., and Hopp, K. (2020). Metabolic reprogramming in autosomal dominant polycystic kidney disease: evidence and therapeutic potential. Clin. J. Am. Soc. Nephrol. *15*, 577–584. https://doi.org/10.2215/CJN.13291019.

Nowak, K.L., Steele, C., Gitomer, B., Wang, W., Ouyang, J., and Chonchol, M.B. (2021). Overweight and obesity and progression of ADPKD. Clin. J. Am. Soc. Nephrol. *16*, 908–915. https://doi.org/10.2215/CJN.16871020.

Nowak, K.L., You, Z., Gitomer, B., Brosnahan, G., Torres, V.E., Chapman, A.B., Perrone, R.D., Steinman, T.I., Abebe, K.Z., Rahbari-Oskoui, F.F., et al. (2018). Overweight and obesity are predictors of progression in early autosomal dominant polycystic kidney disease. J. Am. Soc. Nephrol. *29*, 571–578. https://doi.org/10.1681/ASN.2017070819.

Pei, Y., Obaji, J., Dupuis, A., Paterson, A.D., Magistroni, R., Dicks, E., Parfrey, P., Cramer, B., Coto, E., Torra, R., et al. (2009). Unified criteria for ultrasonographic diagnosis of ADPKD. J. Am. Soc. Nephrol. *20*, 205–212. https://doi.org/10.1681/ASN.2008050507.

Peters, J.C., Wyatt, H.R., Foster, G.D., Pan, Z., Wojtanowski, A.C., Vander Veur, S.S., Herring, S.J., Brill, C., and Hill, J.O. (2014). The effects of water and non-nutritive sweetened beverages on weight loss during a 12-week weight loss treatment program. Obesity *22*, 1415–1421. https://doi.org/10.1002/oby.20737.

Romashkan, S.V., Das, S.K., Villareal, D.T., Ravussin, E., Redman, L.M., Rochon, J., Bhapkar, M., Kraus, W.E., and Group, C.S. (2016). Safety of two-year caloric restriction in non-obese healthy individuals. Oncotarget *7*, 19124–19133. https://doi.org/10.18632/oncotarget.8093.

Sallis, J.F., Haskell, W.L., Wood, P.D., Fortmann, S.P., Rogers, T., Blair, S.N., and Paffenbarger, R.S., Jr. (1985). Physical activity assessment methodology in the five-city project. Am. J. Epidemiol. *121*, 91–106.

Schrier, R.W., Abebe, K.Z., Perrone, R.D., Torres, V.E., Braun, W.E., Steinman, T.I., Winklhofer, F.T., Brosnahan, G., Czarnecki, P.G., Hogan, M.C., et al. (2014). Blood pressure in early autosomal dominant polycystic kidney disease. N. Engl. J. Med. *371*, 2255–2266. https://doi.org/10.1056/NEJMoa1402685.

Sorgente, A., Pietrabissa, G., Manzoni, G.M., Re, F., Simpson, S., Perona, S., Rossi, A., Cattivelli, R., Innamorati, M., Jackson, J.B., et al. (2017). Web-based interventions for weight loss or weight loss maintenance in overweight and obese people: a systematic review of systematic reviews. J. Med. Internet Res. *19*, e229. https://doi.org/10.2196/jmir.6972.

Torres, J.A., Kruger, S.L., Broderick, C., Amarlkhagva, T., Agrawal, S., Dodam, J.R., Mrug, M., Lyons, L.A., and Weimbs, T. (2019). Ketosis ameliorates renal cyst growth in polycystic kidney disease. Cell Metab *30*, 1007–1023. https://doi.org/10.1016/j.cmet.2019.09.012.

Torres, V.E., Harris, P.C., and Pirson, Y. (2007). Autosomal dominant polycystic kidney disease. Lancet *369*, 1287–1301. https://doi.org/10.1016/S0140-6736(07)60601-1.

Torres, V.E., Chapman, A.B., Devuyst, O., Gansevoort, R.T., Grantham, J.J., Higashihara, E., Perrone, R.D., Krasa, H.B., Ouyang, J., Czerwiec, F.S., et al. (2012). Tolvaptan in patients with autosomal dominant polycystic kidney disease. N. Engl. J. Med. *367*, 2407–2418. https://doi.org/10.1056/NEJMoa1205511.

Trepanowski, J.F., Kroeger, C.M., Barnosky, A., Klempel, M.C., Bhutani, S., Hoddy, K.K., Gabel, K., Freels, S., Rigdon, J., Rood, J., et al. (2017). Effect of alternate-day fasting on weight loss, weight maintenance, and cardioprotection among metabolically healthy obese adults: a randomized clinical trial. JAMA Intern. Med. *177*, 930–938. https://doi.org/10.1001/jamainternmed.2017.0936.

Varady, K.A., Bhutani, S., Klempel, M.C., and Kroeger, C.M. (2011). Comparison of effects of diet versus exercise weight loss regimens on LDLand HDLparticle size in obese adults. Lipids Health Dis. *10*, 119. https://doi.org/10.1186/1476-511X-10-119.

Warner, G., Hein, K.Z., Nin, V., Edwards, M., Chini, C.C., Hopp, K., Harris, P.C., Torres, V.E., and Chini, E.N. (2016). Food restriction ameliorates the development of polycystic kidney disease. J. Am. Soc. Nephrol. *27*, 1437–1447. https://doi.org/10.1681/ASN.2015020132.

Weston, A.D., Korfiatis, P., Kline, T.L., Philbrick, K.A., Kostandy, P., Sakinis, T., Sugimoto, M., Takahashi, N., and Erickson, B.J. (2019). Automated abdominal segmentation of ct scans for body composition analysis using deep learning. Radiology *290*, 669–679. https://doi.org/10.1148/radiol.2018181432.

STAR★METHODS

KEY RESOURCES TABLE

REAGENT or RESOURCE	SOURCE	IDENTIFIER
Antibodies		
Rabbit monoclonal anti p-AMPKα	Cell Signaling Technology	Cat #2535; RRID:AB_331250
Rabbit monoclonal anti AMPKα	Cell Signaling Technology	Cat #5832; RRID:AB_10624867
Mouse monoclonal anti p-p70 S6	Santa Cruz Biotechnology	Cat #sc-8416; RRID:AB_2182257
Rabbit monoclonal anti p70 S6	Cell Signaling Technology	Cat #2708; RRID:AB_390722
Rabbit monoclonal anti S6	Cell Signaling Technology	Cat #2217; RRID:AB_331355
Rabbit monoclonal anti p-S6	Cell Signaling Technology	Cat #5364; RRID:AB_10694233
Rabbit monoclonal anti AMPKα	Cell Signaling Technology	Cat #5831; RRID:AB_10622186
Rabbit monoclonal anti LKB1	Cell Signaling Technology	Cat #3047; RRID:AB_2198327
Rabbit monoclonal anti p-LKB1	Cell Signaling Technology	Cat #3482; RRID:AB_2198321
Rabbit monoclonal anti SirT1	Cell Signaling Technology	Cat #9475; RRID:AB_2617130
Rabbit polyclonal anti LC3A/B	Cell Signaling Technology	Cat #4108; RRID:AB_2137703
Rabbit polyclonal anti SQSTM1/p62	Cell Signaling Technology	Cat #5114; RRID:AB_10624872
Rabbit polyclonal anti GAPDH	Santa Cruz Biotechnology	Cat #sc-25778; RRID:AB_10167668
Rabbit monoclonal anti β-Actin	Cell Signaling Technology	Cat #4970; RRID:AB_2223172
Biological samples		
PBMCs	This manuscript	Prospectively collected
Chemicals, peptides, and recombinant proteins		
Teklad global 19% protein extruded rodent diets	ENVIGO	Cat #2019
Critical commercial assays		
IGF-1 ELISA	R & D systems	Cat # DG100B
IGFBP-1 ELISA	R & D systems	Cat # DGB100
CRP V-plex	Meso Scale Discovery	K151STD
Leptin, ghrelin, IL-6, IL-18, RNF-a, MCP-1 U-plex	Meso Scale Discovery	Customized kit
QuantiChrom Urea Assay Kit	BioAssay Systems	Cat #DIUR-100
Deposited data		
Human Data	Zenodo	https://doi.org/10.5281/zenodo.5770457
Experimental models: Organisms/strains		
C57Bl/6J F3 Pkd1RC/RC	Hopp et al., 2015	Pkd1tm1.1Pcha MGI (http://www.informatics.jax.org/)
Software and algorithms		
Analyze 11.0	Analyze Direct	https://analyzedirect.com/
SAS version 9.4	SAS Institute	https://www.sas.com
SPSS version 27.0	IBM	https://www.ibm.com/spss/statistics
GraphPad Prism	GraphPad	https://graphpad.com
MatLab 2015b	MathWorks	https://www.mathworks.com/?s_tid=gn_logo
JMP Pro 15	SAS Institute	https://www.jmp.com/en_us/
ParaVision NEO360	Bruker	N/A
NIS-Elements AR v4.6	Kleczko et al., 2018	N/A
ImageJ	Kleczko et al., 2018	https://imagej.nih.gov/ij/
"PyCysticImage" package	This manuscript	https://github.com/TLKline/PyCysticImage

(*Continued on next page*)

Continued

REAGENT or RESOURCE	SOURCE	IDENTIFIER
Other		
BioDAQ system	Research Diets Inc.	https://researchdiets.com/biodaq
EchoMRI™-100RM	Echo Medical Systems	http://www.echomri.com/

RESOURCE AVAILABILITY

Lead contact

Further information and requests for resources and reagents should be directed to and will be fulfilled by the lead contact, Kristen Nowak (Kristen.Nowak@cuanschutz.edu).

Materials availability

This study did not generate new unique reagents or mouse lines. Mouse tissue generated through the study will be made available with the appropriate MTA.

Data and code availability

- De-identified human data have been deposited at Zenodo, and accession number is listed in the key resources table. They are available upon request if access is granted. To request access, contact the lead author.
- All original code has been deposited at GitHub and is publicly available as of the date of publication. DOIs are listed in the key resources table.
- Any additional information required to reanalyze the data reported in this paper is available from the lead contact upon request.

EXPERIMENTAL MODEL AND SUBJECT DETAILS

Human study

Eligible participants were enrolled at the University of Colorado Anschutz Medical Campus between June 2018 and August 2019 (the trial concluded according to enrollment determined by the protocol). Details regarding age, sex of participants, and included sample size are provided in the Results.

All procedures were approved by the Institutional Review Board of the University of Colorado Anschutz Medical Campus (protocol #17-1327) and adhere to the *Declaration of Helsinki*. The nature, benefits, and risks of the study were explained to the volunteers and their written informed consent was obtained prior to participation. The study protocol is provided as a Supplementary method, related to STAR methods.

The study aimed to recruit 30 participants across three smaller cohorts. Each cohort had baseline measurements and randomization at approximately the same time to conduct the behavioral intervention in a group setting. Randomization was 1:1 (DCR:IMF) with a blocked randomization sequence with stratification by sex.

Animal study

All animal procedures were performed in an AAALAC-accredited facility in accordance with the *Guide for the Care and Use of Laboratory Animals* (Institute of Laboratory Animal Research, 2011) and approved by the University of Colorado Anschutz Medical Campus Institutional Animal Care and Use Committee (protocol #301). Fully inbred, homozygous C57Bl/6J*Pkd1*$^{RC/RC}$ mice were obtained from the Mayo Clinic in 2015 with an approved MTA and were maintained in homozygosity by the study PI, Katharina Hopp (Arroyo et al., 2021; Hopp et al., 2012, 2015). Homozygous C57Bl/6J*Pkd1*$^{RC/RC}$ mice were outcrossed every 10th generation to wildtype C57Bl/6J mice obtained from *The Jackson Laboratory* (stock number #000664). All animals included in this study were from a third generation backcross and their genotype was confirmed as previously published (Hopp et al., 2012; Kleczko et al., 2018). Both sexes, males and females, were utilized for the study.

From birth until 24 days of age mice were housed with their parents. At 24 days of age mice were weaned together with same sex/age mice that were part of the study: 3–5 mice/cage. Until 11 weeks of age mice were housed in the main vivarium facility, which maintains a temperature of ~72ºF, humidity of ~37%, and light cycle of 8 pm off, 6 am on. At 11 weeks of age, all experimental animals were transferred to the Nutrition Obesity Research Center (NORC) facility (temperature: ~80ºF, humidity: ~35%, light cycle: 4pm off, 2am on). Here, they were placed into singly housed, wire bottom cages with gated food hoppers. Mice could acclimate to this new housing setup for one week prior study start. All cages were sterile, and animals received hyperchlorinated reverse osmosis water delivered via an automatic watering system and irradiated diet (ENVIGO #2019, 45% carbohydrate, 19% protein, 9% fat) to closely parallel the intake regimens of the human trial participants.

Before study start and at the end of study, animals underwent pathogen testing and tested negative for the following by serology: Mouse hepatitis virus (MHV), Mouse minute virus of mice (MVM), Mouse rotavirus (MRV/EDIM), Mouse parvovirus (MPV), Mouse norovirus (MNV), Theiler's murine encephalomyelitis virus (TMEV), Sendai virus (SEND), *Mycoplasma pulmonis*, Reovirus type 3 (REO3), Polyoma, Mouse adenovirus 1 (MAV1), Mouse adenovirus 2 (MAV2), Ectromelia virus, lymphocytic choriomeningitis virus (LCMV). Mice also tested negative for the following by PCR: *Corynebacterium bovis*, Pinworms (*Syphacia obvelata*, *Syphacia muris*, *Aspiculuris tetraptera*) and Fur Mites (*Myocoptes*, *Myobia* and *Radfordia* spp.).

METHOD DETAILS

Human study

Overview of experimental design. A 1-year, randomized, two-active-arm, single-blind pilot study with dietary restriction was conducted with a primary aim of determining the feasibility of delivering a 1-year behavioral weight loss intervention (based on either DCR or IMF) in adults with overweight or obesity and ADPKD with normal to moderately declined kidney function. Subjects were recruited nationally and underwent telephone and laboratory screening for inclusion/exclusion criteria (described below) and were then randomly assigned to either DCR or IMF. Members of the investigative team involved in the acquisition and analysis of data were blinded to the treatment status. Due to the nature of the intervention, study participants were not blinded. Both groups received a comprehensive, group-based, behavioral, weight loss intervention. Randomized groups met virtually and separately in small cohorts via the web-based platform Zoom (HIPAA compliant).

Inclusion and exclusion criteria. Participants eligible for inclusion were men and women 18–65 years of age with ADPKD based on the updated Ravine criteria (Pei et al., 2009). Baseline BMI was 25–45 kg/m^2 and baseline eGFR was $\geq$30 mL/min/1.73m^2 by the Chronic Kidney Disease Epidemiology Collaboration (CKD-EPI) equation (Levey et al., 2009). Participants had access to the internet with video chat capabilities, no plans for extended travel without internet access (for >2 weeks) during the 3-month intensive period, and were not participating in another weight loss program.

Participants were excluded if they had diabetes mellitus (diagnosis, fasting glucose $\geq$126 mg/dL or HbA1C $\geq$ 6.5%), current nicotine use or history of use in the past 12 months, alcohol or substance abuse (self-report or undergoing treatment), history of hospitalization or major surgery within the last 3 months, untreated dyslipidemia (LDL cholesterol >190 mg/dL or triglycerides >400 mg/dL), or uncontrolled hypertension (SBP >160 mmHg or DBP >100 mmHg). Women could not be pregnant, lactating, or unwilling to use adequate birth control. Participants were also excluded if they had a history of cardiovascular disease, peripheral vascular disease, cerebrovascular disease, significant pulmonary disorders (including chronic obstructive pulmonary disease, interstitial lung disease, cystic fibrosis, or uncontrolled asthma), significant gastrointestinal disease (including chronic malabsorptive conditions, peptic ulcer disease, Crohn's disease, ulcerative colitis, chronic diarrhea, or active gallbladder disease), cancer (within the last five years, except for skin cancer or other cancers considered cured with excellent prognosis), or untreated hypo- or hyperthyroidism (thyroid-stimulating hormone outside of normal range for laboratory or history of uncontrolled thyroid disorder; history of thyroid disorder or current thyroid disease treated with stable medication regimen for at least 6 months was acceptable).

Additional exclusion included an abnormal resting electrocardiogram (serious arrhythmias, including multifocal premature ventricular contractions (PVCs), frequent PVCs (defined as 10 or more per min), ventricular tachycardia (defined as runs of 3 or more successive PVCs), or sustained atrial tachyarrhythmia; second or third degree A-V

block, QTc interval >480 msec or other significant conduction defects), regular use of prescription or over-the-counter medications that may affect weight, appetite, food intake, or energy metabolism (e.g., appetite suppressants, lithium, stimulants) or regular use of obesity pharmacotherapeutic agents within the last 6 months, weight loss >5% in the past three months for any reason except post-partum weight loss, weight gain >5% in the past 3 months, or history of a clinically diagnosed eating disorder including anorexia nervosa, bulimia (binge eating disorder score >20 on the Eating Attitudes Test (EATS-26)) (Garner et al., 1982) required further assessment by the Study MD to determine if it is appropriate for the subject to participate in the study. Current severe depression or history of severe depression within the previous year, based on DSM-IV-TR criteria for Major Depressive Episode or score >18 on the Beck Depression Inventory (Beck et al., 1988) required further assessment by the Study MD to determine if it was appropriate for the subject to participate in the study. Finally, participants were excluded if they had a history of other significant psychiatric illness (psychosis, schizophrenia, mania, bipolar disorder) which in the opinion of the Study MD would interfere with their ability to adhere to dietary interventions. Individuals with an inability to cooperate with/clinical contraindication for MRI including severe claustrophobia, implants, devices, or non-removable body piercings were not included in this procedure but could still enroll in the study. Prevalent tolvaptan usage was not exclusionary, although no participants that enrolled were using tolvaptan.

Dietary restriction intervention. The behavioral weight loss interventions were administered by the Colorado Nutrition and Obesity Research Center (NORC) Clinical Intervention and Translation (CIT) Core. Curriculum for the DCR group was based on the Colorado Weigh behavioral weight loss program, which employs a skills-based approach and cognitive behavioral strategies toward lifestyle modification (Peters et al., 2014). Curriculum for the IMF intervention was developed by Dr. Catenacci and a Registered Dietician (RD) to include similar themes to DCR, but with focused behavioral support for IMF. Sessions for each group were taught by an RD experienced with group-based behavioral interventions. The initial 3 months was an intensive phase with weekly sessions focusing on achieving initial weight loss. The final 9 months focused on weight loss maintenance with monthly sessions focusing on strategies to maintain the weight loss achieved in the first 3 months. Format included a mix of large-group discussion, small breakout discussions, visual demonstrations, and written exercises. Topics included: realistic weight loss goal setting, self-monitoring strategies, mindful eating, stress management, cognitive restructuring, and strategies to overcome barriers to healthy eating. Specific topics related to DCR and IMF were also covered in each respective group. IMF-specific strategies included: strategies to deal with hunger on fast days, distraction techniques, and choosing a balanced diet/appropriate portions on fed days. Maintenance phase topics included: overcoming weight loss plateaus, screen time and sedentary behavior, negative self-talk, cooking demonstrations, and guest speakers. Participant weight was also tracked weekly at the time of these sessions by a BodyTrace scale for secure remote transmission of body weight to facilitate RD guidance.

Both groups reduced overall energy intake by ~34% per week, using either DCR or IMF. Recommended macronutrient content (55% carbohydrate, 15% protein, 30% fat) was the same in both groups. The goal of the DCR group was a ~34% daily energy deficit from baseline individual weight maintenance energy requirements (based on resting energy expenditure x activity factor of 1.5), which was measured between 6 and 10 AM after rest and 24-h abstention from exercise using standard indirect calorimetry (Grunwald et al., 2003) with the ventilated hood technique. Participants in this group were also instructed in specific strategies to support DCR, including counting calories, portion size awareness, and daily food logging.

Participants in the IMF group were instructed to reduce energy intake to ~20% of estimated energy requirement (determined as described above), delivered as a single meal on three non-consecutive days per week, resulting in a weekly energy deficit of ~34% (similar to the DCR group). Sample fast day menus and individualized fast day calorie goals were provided to assist with achieving energy intake targets. On fast days, participants were allowed to consume their calories at the meal of their choice, as a previous study using a similar IMF protocol found that altering times of caloric intake during the modified fast day did not impact weight loss or compliance (Hoddy et al., 2014). On fed days, IMF participants ate *ad libitum*, but were encouraged to make healthy food and portion choices. Participants in this group were instructed in calorie counting but were asked to count calories and log food intake only on fast days on a weekly basis. They were also instructed in specific strategies to support IMF, as described above.

We elected to use a two-active-arm study design because neither weight loss nor periods of fasting had been evaluated previously in humans with ADPKD. Thus, a comparison of IMF to weight loss resulting

from a traditional DCR approach was merited. While a control group was considered, given that the primary outcome of this pilot study was feasibility, it was determined that two active groups was a more valuable design than including a control group (including review by an NIH study section). The study duration of the intensive phase (3 months) was selected to achieve ~5% weight loss based on the duration of numerous previous pilot and feasibility studies in overweight and obese adults without ADPKD (Johnson et al., 2007; Varady et al., 2011; Klempel et al., 2010; Catenacci et al., 2016), length of animal studies showing changes in biological pathways (Warner et al., 2016; Kipp et al., 2016), and to inform a large-scale randomized controlled trial. The 9-month maintenance phase was selected to provide preliminary insight into percent change in htTKV at 12 months with each weight loss approach.

Participants were not withdrawn by the PI for non-adherence in this intent-to-treat study. Participants were encouraged to adhere to the dietary prescriptions for the initial 2 weeks as a prior study suggests individuals with obesity become habituated to IMF after ~2 weeks (Klempel et al., 2010). After the initial 2 weeks, a standardized dietary modification was offered if a participant: (1) expressed a desire to withdraw due to intolerance of study diet and/or (2) experienced adverse effects related to the study diet (i.e., insomnia, impaired concentration, irritability) that impair ability to function. The percentage of participants in each group requiring intervention modification was recorded.

Because of the COVID-19 pandemic and Institutional and state policies in place, the length of treatment of numerous participants was extended with IRB approval. Participants continued with virtual group sessions on a monthly basis during this period and their end-of-study visit was scheduled at the earliest appropriate time point and was considered in the analysis as month 12.

Outcome measures

Feasibility. Careful records were kept regarding numbers of individuals pre-screened, screened, enrolled, and completed in order to evaluate feasibility. Body weight was measured on a calibrated digital scale to the nearest 0.1 kg and height was measured to the nearest 1 mm using a stadiometer at baseline and 12 months at the University of Colorado PKD research clinic. Body weight was also collected remotely at the times of group web-based sessions using BodyTrace scales to guide these sessions. Percent weight loss and BMI were calculated at baseline, 3 months, and 12 months. If a final weight was not available at month 12, the last weight available after month 6 via BodyTrace measurements was used in these calculations. Waist and hip circumference were also measured at baseline and 12 months.

Safety, acceptability, and tolerability. Fasting blood samples were collected for screening and repeated at 3 and 12 months for analyses including a CMP, CBC, HbA1c, lipid panel, and TSH. Samples were collected the morning following a fed day for the IMF group to avoid the acute effects of fasting. Estimated GFR was calculated using the CKD-EPI equation (Levey et al., 2009). Month 3 samples were collected at a contract laboratory for all non-local participants. A pregnancy test was performed in all premenopausal women at baseline. A standard physical exam and medical history were administered by a physician, and a resting 12-lead electrocardiogram was performed (baseline and month 12). Blood pressure (Omron HEM 907XL) and other vital signs were also measured at baseline and month 12, and via home blood pressure monitors monthly (A&D UA-611). Self-reported dietary adherence, effort to adhere, and self-efficacy to adhere were assessed monthly using a 1–10 Likert scale (Dansinger et al., 2005).

Participants were encouraged to report adverse events to study staff as they occurred and were also asked about adverse events via monthly phone calls. Additional parameters to assess tolerability were collected at baseline and months 3 and 12 as follows: Quality of life (QOL) was assessed with the RAND 36 Item Health Survey (RAND-36) (Hays and Morales, 2001) physical and mental health component summary score. Mood state was assessed with the Profile of Mood States 2 (POMS-2) (Mcnair et al., 1971). Binge eating behavior was assessed with the Questionnaire on Eating and Weight Patterns-Revised (QEWP-5) (Nangle et al., 1994). Additionally, to gain insight into physical activity, self-reported physical activity was quantified at baseline, 3, and 12 months using the Stanford Physical Activity Questionnaire (Sallis et al., 1985).

Circulating markers. Serum IGF-1 (1:100 dilution, DG100B, R&D systems), IGFBP-1(1:10 dilution, DGB100, R&D systems), adiponectin (1:100 dilution, DRP300, R&D systems), CRP (1:1,000, V-plex, K151STD, Meso Scale Discovery), leptin, ghrelin, IL-6, IL-18, TNF-α, MCP-1, and insulin (1:2 dilution, Customized U-Plex Metabolic Group 1, Meso Scale Discovery) were measured at baseline and 12 months

using fasting blood samples. Insulin resistance was estimated with the HOMA-IR formula (Matthews et al., 1985). Some participants also had successful remote 3-month samples returned, although this was limited by contract laboratory protocol adherence and COVID-19. Samples were collected the morning following a fed day for the IMF group to avoid acute effects of fasting.

PBMC isolation and western blot analysis. PBMCs were isolated from heparinized whole blood using serum-separating vacutainers and Ficoll Hypaque-containing cell preparation tubes with sodium citrate (CPT Vacutainer, BD, Franklin Lakes, NJ, USA) for the separation of PBMCs from whole blood (Brunt et al., 2018). The PBMCs were washed and lysed in lysis buffer containing RIPA buffer (#89900, Thermo Scientific) with protease inhibitor (#P8340, Sigma Aldrich) and phosphatase inhibitor (#A32955, Thermo Scientific). Protein concentration was measured using DC protein assay (#5000111, Bio-Rad). The protein samples were loaded on 4–15% gradient Criterion TGX pre-cast gels (Bio-Rad, #5671083) and transferred to PVDF membranes. The membrane was blotted with 5% BSA followed by incubation/blotting with primary antibodies of phospho-AMPK (Thr172) (1:200, #2535, Cell Signaling Technology) and AMPK (1:300, #5832, Cell Signaling Technology), phospho-p70 S6 (1:200, SC-8416, Santa Cruz Biotechnology) and p70 S6 (1:500, #2708, Cell Signaling Technology) (De Kreutzenberg et al., 2015) and β-actin (1:2000, #4970, Cell Signaling Technology). Goat anti-rabbit (#7074, Cell Signaling Technology) and horse anti-mouse (#7076, Cell Signaling Technology) HRP-conjugated secondary antibodies were used against the above primary antibodies. The membranes were exposed to ECL reagent (#34094, SuperSignal West Femto, Thermo Scientific) and scanned using UVP ChemStudio Western blot imager system (Analytik Jena). Band density of each blot was quantified using ImageJ software. Samples were collected the morning following a fed day for the IMF group to avoid acute effects of fasting.

Abdominal MRI. A Siemens Skyra 3.0 T system was used to obtain an abdominal MRI at baseline and 12 months, in a similar manner described for the CRISP study (Grantham et al., 2006). No contrast agents were used. TKV was measured using Analyze software (Analyze 11.0, Mayo Foundation, Rochester, MN) by a single blinded investigator. Annual percent change in htTKV was calculated based on actual number of months between baseline and end-of-study MRI acquisition. Disease severity was categorized according to the Mayo Imaging Classification system (Irazabal et al., 2015). Cystic index was determined using an automated deep learning approach (Kline et al., 2020). We also adapted a methodology to measure abdominal adiposity by CT (Weston et al., 2019) to differentiate SAT, muscle, VAT, visceral organ, and bone compartments using MRIs acquired as part of the assessment of TKV. The technique used the T2-weighted MRI oriented in the axial plane with slice level at the L3 vertebra to segment and, thereby, differentiate the compartments. The segmentations/tracings of the individual compartments were performed manually using an in-house software annotation tool (Kline et al., 2016). From this, regional measurements of both area (2D) and volume (3D) can be used to quantify various body composition parameters. Using this technique, abdominal adiposity (SAT, VAT, and total AT) was quantified. The "PyCysticImage" package consisting of image processing tools is publically available through GitHub (https://github.com/TLKline/PyCysticImage).

Sample size estimation. The sample size was determined to evaluate the feasibility of enrolling, retaining, and performing outcome measurements in a number of participants equal to a single cohort in a future large-scale trial. The cohort size was also ideal for a remotely conducted group-based lifestyle weight loss intervention, allowing for optimal group dynamics as well as individualized attention from the RD. Additionally, a total of 12 participants (accounting for 20% drop-out) per group would afford 99% power at an *alpha* level of 0.05 to detect weight loss of >5% (−6.2 ± 0.9%) (Catenacci et al., 2016) in each group (note, we did not hypothesize significantly different weight loss between groups, thus between group power calculations were not performed, and this comparison is to no weight loss).

Animal study

Experimental design and dietary intervention. For this study, C57Bl/6J*Pkd1*$^{RC/RC}$ mice were singly housed in wire bottom cages equipped with computer-controlled, gated food hoppers, hindering coprophagy and allowing precise regulation of feeding times/amounts, respectively. In this housing environment, we first established daily baseline *ad libitum* (AL) food intake of F3 C57Bl/6J*Pkd1*$^{RC/RC}$ mice for two weeks and found males (M) to consume 2.0g ± 0.28g and females (F) to consume 1.8g ± 0.15g of food (N = 3/sex).

All study animals (F3 C57Bl/6J*Pkd1*$^{RC/RC}$ mice) first underwent MRI (study start) at 11 weeks of age and then were transferred from their normal housing facility to the NORC facility, where they underwent QMR (study start). Body weight (BW) was also measured at study start. Group assignment was not based on the initial parameters (MRI/QMR analyses or BW), but same sex littermates were randomly distributed among the different dietary intake groups. From 11 weeks of age to 12 weeks of age animals could acclimate to their new housing facility, which included feeding out of a hopper attached to the outside of their singly housed wire-bottom cage. During the one-week acclimation, the gate to the food hopper was open continuously. When the mice reached 12 weeks of age the BioDAQ system (Research Diets Inc.) was activated. The system recorded episodic food intake and allows automatic hopper gate opening/closing. For animals in the AL feeding group, the hopper gates remained continuously open throughout the study and food intake per cage/per animal was recorded daily. For animals on the DCR dietary regimen, the allowed food intake was set to 1.4g daily for males (M, N = 4) and 1.26g daily for females (F, N = 3; 70% of AL [M = 2.0g/daily (N = 8), F = 1.8g/daily (N = 4)], as determined before study start in a separate cohort of F3 C57Bl/6J*Pkd1*$^{RC/RC}$ mice). For animals on DCR, the food hopper gate opened at 6 pm and closed once the daily allotted amount of food was consumed, which took on average 0.5–3h. For animals on TRF (N = 3M, 4F), the hopper gate opened at 6 pm and closed at 2 am. During that time, animals were able to eat *ad libitum*, and daily food intake was recorded. For animals on IMF the allotted food intake on Mondays (Mo), Wednesdays (We), and Fridays (Fr) was set to 0.4g for M (N = 4) and 0.36g for F (N = 5, 20% of AL). The food hopper gates for IMF animals opened at 4pm and closed once the allotted food amount was consumed, which on average took 15 min to 2 h. Hopper gates then opened at midnight again for the following *ad libitum* feeding day and remained open for 24 h. Hence, animals fasted from midnight until 4 pm (16h) every alternate date, except Saturday (Sa) and Sunday (Su). On Tuesday (Tu), Thursday (Th), Sa, and Su (midnight until midnight) animals could eat *ad libitum* and food intake was recorded. Food intake was analyzed for the first, second, fourth, eighth, and 12th week of the study (3M, 3F), and BW of all animals was measured at the start of week 1, 2, 4, 8, and 12 and always measured on *ad libitum* days in case of the IMF group. At the end of study (24 weeks of age) animals underwent end of study QMR and MRI and were sacrificed for detailed evaluation.

Outcome measures

Mouse tissue harvest/analysis. Mice were euthanized by an isoflurane overdose using an isoflurane chamber followed by cervical dislocation. Following euthanasia BW was recorded and blood was collected via cardiac puncture into a heparin coated tube. Kidneys, liver, heart, spleen, and femur were dissected out and weight or measured in length (femur). Pieces of each tissue were fixed in 4% paraformaldehyde or flash frozen in liquid nitrogen. Tissue fixed in paraformaldehyde was processed and embedded in paraffin and sectioned at 4μm for histological analyses.

Histomorphometric analyses. For each animal, the left kidney was analyzed by histomorphometry. Three kidney cross sections were analyzed per kidney/animal: One of the superior pole, one of the inferior pole, and one across the renal pelvis. Sections were stained by H&E and picrosirius red. Cystic index, cyst size, and number were analyzed using a custom-built NIS-Elements AR v4.6 macro (Nikon). A cyst was defined as having a minimum Feret diameter of 50 μm. The cystic index was defined as the percentage of cystic area per kidney cross section, and cyst number was normalized to area. Fibrotic area was analyzed from picrosirius red stained kidney sections and visualized using an Olympus BX41 microscope with a linear polarizer. Six random cortical 40x images were analyzed per animal and the percent fibrotic area was calculated from each image. Fibrillar collagen (birefringent area) was quantified using ImageJ. Computed cystic volume and computed fibrotic volume were determined by multiplying the percent cystic or fibrotic area by the two-kidney weight.

Kidney function analysis. Blood urea nitrogen levels were measured from blood harvested via cardiac puncture at time of sacrifice using the QuantiChrom Urea Assay Kit (DIUR-100, BioAssay Systems), following the manufacturer's protocol. Five μL of plasma from the terminal blood collection were analyzed per sample and all animals were analyzed in duplicates.

Magnetic resonance imaging. *In vivo* MRI was performed on anesthetized mice (2.5% isoflurane) using a 9.4 Tesla BioSpec animal MRI scanner (Bruker Medical, Billerica, MA) and a bird-cage mouse body coil. After obtaining tri-pilots for kidney localization, optimized proton density-weighted (PDw) rapid acquisition with relaxation enhancement (RARE) scans with fat suppression were acquired for the volumetric assessment of both kidneys. To quantify the relative cyst volume, trueFISP (fast imaging with steady state free

precession) scans were then obtained. All images were acquired in transversal and coronal planes using the following optimized parameters: field of view 40 × 40 mm^2; slice thickness 1 mm; matrix size 256 × 256; TR/TE = 2,600/8 ms (PDw RARE) and 5/2.5 ms (FISP); flip angle 90/180° (PDw RARE) and 60° (FISP). Total acquisition time for all sequences was 16 min57 s.

TKV was quantified by placing hand-driven region of interest (ROI) on each anatomical slice for the right and left kidney, summing and multiplying by the slice thickness (reported in mm^3) using Bruker ParaVision *NEO*360 software. Signal intensity (SI) histograms were generated by pixel-wise fitting using in-house developed software in MATLAB (MathWorks, Natick, MA, USA, version 2015b). Processing was performed separately for each kidney and consisted of semi-automated segmentation, SI histogram generation and model fitting. The cyst and kidney segmentation volumes were reported (%) using a reader-determined cut-off values for a cyst-related SI index.

Quantitative magnetic resonance analyses. Body composition was measured on live mice prior to the start of study and at the end of study utilizing an EchoMRI QMR instrument (EchoMRI-100RM, Echo Medical Systems). Live animals were restrained in the 100g cylindrical holder suitable for mice and placed in the machine for measurement of fat, lean, and free water mass. Measurements took ~3 min per mouse, and an average of three measurements per mouse was utilized for analyses. Body composition was analyzed utilizing the equipment compatible software (EchoMRI v2018).

Western blotting analysis. Mouse kidneys were homogenized in lysis buffer containing RIPA buffer and protease inhibitor (#P8340; Sigma Aldrich). Protein concentration was measured using Protein assay dye reagent concentrate (#5000006, Bio-Rad) which is based on the Bradford method. The protein samples were loaded on 4%–20% gradient pre-cast gels (#4568096; Bio-Rad) and transferred to PVDF membranes. The membrane was blocked with 5% BSA, followed by incubation/blotting with primary antibodies of S6 (#2217L; Cell Signaling Technology, Inc.), phospho-S6 (#5364S; Cell Signaling Technology, Inc.), AMPK alpha (#5831S; Cell Signaling Technology, Inc.), phospho-AMPK alpha (#2535S; Cell Signaling Technology, Inc.), LKB1 (#3047S; Cell Signaling Technology, Inc.), phospho-LKB1 (#3482S; Cell Signaling Technology, Inc.), SIRT1 (#9475T; Cell Signaling Technology, Inc.), LC3-I/II (#4108s; Cell Signaling Technology, Inc.), SQSTM1/p62 (#5114; Cell Signaling Technology, Inc.), and GAPDH (#sc-25778; Santa Cruz Biotechnology, Inc.). The working dilution for all the antibodies was 1:1,000. Goat anti-rabbit HRP conjugated secondary antibody was used against the above primary antibodies (#7074S; Cell Signaling Technology, Inc.). The membranes were exposed to ECL reagent (#NEL104001EA; PerkinElmer) and developed using an X-ray film developer. Band density of each blot was quantified using ImageJ software.

QUANTIFICATION AND STATISTICAL ANALYSIS

Human study

If an outcome variable had more than two measurements, data from month 0 (baseline), 3 months, and 12 months were included in a repeated measure analysis, which was performed by employing a mixed effects model with a time by treatment interaction effect (to assess the treatment effect) and without adjustment for any covariates. The covariance structure used was unstructured covariance structure. Furthermore, the comparisons between time points within a group were performed with Tukey-Kramer adjustment. If an outcome had only two measurements, the independent samples t-test was used to compare the change in the variable between groups. A paired t-test was also used for a pre-post comparison within a group or pooled groups to compare measurements at 12 months to baseline. Proportions of study-related adverse events and questionnaire data were also compared between groups using a least square mean test, Chi-square tests, or Fisher's exact test. Correlations were performed using Pearson's bivariate correlation. Historical data were planned *a priori* to be presented for qualitative comparison regarding change in htTKV. Non-normally distributed variables were log-transformed prior to analysis. There was no adjustment for multiple comparisons as the aim of the study was feasibility rather than efficacy. Alpha was set at 0.05 (two-sided). All data are reported as means ± S.D., medians (interquartile range), or n (%). All statistical analyses were performed by using SAS version 9.4 (SAS Institute, Cary, NC) or SPSS version 27.0 (adherence questionnaires).

Animal study

Data were analyzed using JMP Pro 15 or PRISM9 (GraphPad Software, La Jolla, CA). The graphs depict mean ± SEM. ANOVA followed by Tukey's post-hoc test was used to delineate statistical significance.

For correlation analyses, a Pearson correlation coefficient assuming Gaussian distribution was computed. A $P < 0.05$ was considered significant. An *a priori* power analysis was not performed for determining sample size, but instead prior experience with the model was used to establish a sample size sufficient to delineate therapeutic efficacy. Mice were randomly assigned to the dietary regimens and all data were analyzed in a blinded fashion. No mice were excluded from the study due to health concerns or any other criterion.

ADDITIONAL RESOURCES

The trial was registered at ClinicalTrials.gov (NCT02903511).